

MESOSCALE MODELING OF MECHANICAL RESPONSES IN
POLYMERIC SYSTEMS

BY

PEIJUN YU

BS, University of Shanghai for Science and Technology, 2012

THESIS

Submitted in partial fulfillment of the requirements for
the degree of Master of Science in Mechanical Engineering
in the Graduate School of
Binghamton University
State University of New York
2016

ProQuest Number: 10134298

All rights reserved

INFORMATION TO ALL USERS

The quality of this reproduction is dependent upon the quality of the copy submitted.

In the unlikely event that the author did not send a complete manuscript and there are missing pages, these will be noted. Also, if material had to be removed, a note will indicate the deletion.



ProQuest 10134298

Published by ProQuest LLC (2016). Copyright of the Dissertation is held by the Author.

All rights reserved.

This work is protected against unauthorized copying under Title 17, United States Code
Microform Edition © ProQuest LLC.

ProQuest LLC.
789 East Eisenhower Parkway
P.O. Box 1346
Ann Arbor, MI 48106 - 1346

© Copyright by Peijun Yu 2016

All Rights Reserved

Accepted in partial fulfillment of the requirement for
the degree of Master of Science in Mechanical Engineering
in the Graduate School of
Binghamton University
State University of New York
2016

May 05, 2016

Xin Yong, Chair and Faculty Adviser
Department of Mechanical Engineering, Binghamton University, State University
of New York

Congrui Jin, Member
Department of Mechanical Engineering, Binghamton University, State University
of New York

Changhong Ke, Member
Department of Mechanical Engineering, Binghamton University, State University
of New York

Abstract

For studying the mechanical responses of high molecular polymeric systems under uniaxial tension, we developed a mesoscale model to simulate and analyze the fracture behavior of bulk polymers and double layer cross-linked hydrogels generated by atom transfer radical polymerization (ATRP) in the framework of dissipative particle dynamics (DPD). We first validate the bond breaking model in the single-chain model and then apply the model to explore the mechanical behavior of the bulk polymers and two-layered hydrogels. With 50% of solvent, the bulk polymers are flexible as the polymer chains have freedom of movement. The bonds in the bulk system do not elongate much even the system is highly deformed. The two-layered hydrogels act tougher than the bulk polymers. In the two-layered hydrogel, the structure of polymer network determines the strength at small deformation when the chain movements are restricted and the bond properties determines the strength after the yield happens.

Table of Contents

List of Tables	vi
List of Figures	vii
List of Abbreviations	ix
1. Introduction.....	1
2. Modeling Polymerization Reactions via DPD	3
2.1 Dissipative Particle Dynamics	3
2.2 Atom Transfer Radical Polymerization	7
3. Fracture Model.....	14
3.1 Harmonic Bond.....	14
3.2 Bond breaking model.....	16
4. Equilibration at Constant Pressure.....	21
5. Results.....	22
5.1 Simplified Single-Chain System.....	23
5.2 ATRP Bulk Polymers without Cross-links.....	30
5.2.1 Bulk Polymers Under Stretch and No Bond Breakage.....	32
5.2.2 Bulk Polymers Under Stretch and Bond Breakage.....	33
5.2 Two-Layered Composite Hydrogels with Cross-links	39
6. Conclusion	50
7. Reference	53

List of Tables

Table 1 Species in ATRP	9
Table 2 Parameters for single-chain systems.....	23
Table 3 Parameters for bulk polymers formed using ATRP.....	30
Table 4 Parameters for two-layered hydrogels with cross-linking	40

List of Figures

Figure 1 Initiation scheme of ATRP	9
Figure 2 Propagation scheme of ATRP	10
Figure 3 Cross-linking scheme of ATRP	10
Figure 4 Potential energy for harmonic bonds.....	15
Figure 5 Bond force for harmonic bonds	16
Figure 6 Flow chart of bond breaking.....	18
Figure 7 Pressure profile of pure solvent sample.....	24
Figure 8 Origin and final structure of single-chain model.....	25
Figure 9 Volume, pressure, temperature profile	26
Figure 10 Snapshots of continuous movement of broken chain	27
Figure 11 Probability curve	28
Figure 12 Bulk polymerization at conversion of 90%	29
Figure 13 Bulk polymer at conversion of 15% and 50%	31
Figure 14 Average bond length, maximum bond length and temperature profile.....	32
Figure 15 Volume change under stretch	33
Figure 16 Average, maximum bond length and temperature curve with 1.0 sensitivity..	34
Figure 17 Bond number profile of 1.0 sensitivity.....	35
Figure 18 Volume profile of sample with 1.0 sensitivity	35
Figure 19 Bond number of bulk with 0.9 sensitivity	36

Figure 20 Bond number, average, maximum bond length and temperature profile.	36
Figure 21 Volume profile of sample with 0.9 sensitivity.	38
Figure 22 Double-layered hydrogel.	39
Figure 23 Volume profile of NPT equilibrium.	41
Figure 24 Bond and temperature information of NPT.	42
Figure 25 Bond number of double layer hydrogel under deformation.	43
Figure 26 Bond length and temperature.	44
Figure 27 Pressure curve of hydrogel composites.	44
Figure 28 Density profile.	45
Figure 29 Strain-Stress curve.	47

List of Abbreviations

r_i	Position vector of particle
v_i	Velocity vector of particle
F_i	Force on a particle
F_{ij}^C	Conservative force
F_{ij}^D	Dissipative force
F_{ij}^R	Random force
a_{ij}	Repulsion parameter of conservative force
r_{ij}	Distance between pairwise particles
\hat{r}_{ij}	Unit vector of distance between particles
r_C	Cutoff radius of DPD force
γ	Dissipative coefficient
σ	Dissipation fluctuation coefficient
w^D	Weight function of dissipative force
v_{ij}	Relative velocity of pairwise particles
w^R	Weight function of random force
k_B	Boltzmann constant
T	Temperature
m	Mass of particles
E	Potential energy of harmonic bond
K	Elastic constant of harmonic bond
r	Bond distance

r_0	Equilibrium bond distance
P_b	Probability of bond breaking
ν	Bond frequency
U_0	Basic bond energy
F_{ext}	Net external force acting on bond
γ_0	Bond sensitivity
F_k^i	Force components of particles
C_k^i	Coordinate components of particles
ρ	Number density of model
P	Pressure of the system
N	Number of particles
V	Volume of simulation box

1. Introduction

A hydrogel is a three-dimensionally cross-linked hydrophilic polymer network that can absorb and retain a significant amount of water, up to thousands of times its dry weight. These kinds of hydrogels have excellent biocompatibility and stimulus-response properties, which make them promising for applications like tissue engineering for living organisms or drug delivery (Meakin, 1991).

An essential goal in materials engineering is defining the mechanical properties of materials. The deformation and fracture of materials are two of the most important properties that are of wide interest. Hydrogels are widely used in replacement of body tissues which should experience large load or deformation frequently and for long durations. Some of them must have high uniaxial tensile strength or great ductility and toughness. Experiments are by far the most widely used approach to obtain the mechanical properties of materials. But the regular experiments of testing the tensile strength can not be applied to the hydrogels easily (Yang, Cui, & Qu, 2014). Therefore, it will be beneficial for determination of the mechanical properties of hydrogels if we can predict the mechanical responses and the fracture

behavior of the polymer-solvent model computationally before we actually synthesize and fabricate them. By probing the void areas of models, the simulation can predict the approximate position and time of failure of specific hydrogels.

It is known that the polymerization and de-polymerization are led by the formation and rupture of strong chemical bonds (carbon-carbon covalent bonds specifically in this thesis) in the polymer chains (Lorenz, Stevens, & Wool, 2004). Here we have two major simulations. One is modeling bulk polymers and two-layered hydrogels with double network interface with atom transfer radical polymerization (ATRP) (Yong, Simakova, et al., 2015), the other is modeling the polymer fracture through simulating the deformation and bond breaking of polymer chains.

This thesis is aiming on studying the mechanical responses of polymer-solvent systems under deformation with bond breaking model to observe and analyze the polymer fracture and failure corresponding to different polymer networks and parameters in mesoscale via dissipative particle dynamics (DPD). By the works done in this thesis, we have more detailed understanding of mechanical characteristics of polymer-solvent systems, specifically, hydrogels in the aspects of chemical bonds or physical entanglements.

2. Modeling Polymerization Reactions via DPD

2.1 Dissipative Particle Dynamics

The three-dimensionally cross-linked hydrogel with hydrophilic polymer networks combined with solvent as well as a large amount of systems of academic and industrial interest are examples of soft condensed matter. These soft condensed matters are neither completely solid nor pure liquid. In the polymer-solvent system used here, we have the spring-bead model of polymer chains with harmonic bonds (Groot & Warren, 1997).

The polymer modeling samples used in this thesis are modeled via dissipative particle dynamics (DPD). DPD can be considered as a coarse-grained molecular dynamics method. It has the similarity to molecular dynamics (MD) method that we can examine larger system at longer time length in computationally realistic timeframes. These characteristics make DPD a relatively more effective way to simulate all the complex polymeric systems in this thesis in mesoscale method.

Recently there are few DPD approaches that incorporate the interactions between polymer networks and solvent in complex gel systems with pure physical entanglements or chemically cross-linked hydrogel systems. The

complexity of the systems makes it difficult to realistically model hydrogels. The starting point of this analysis will be the formulation of DPD, who studied the fluctuation-dissipation theorem in connection with this method. In the formulation they introduced, there is a three-force combination as the interaction force between all the particles. Those three forces are: a conservative force F_{ij}^C , a dissipative force F_{ij}^D and a random force F_{ij}^R . The random forces and dissipative forces have to follow a specific relationship so that the system under simulating will have the statistical mechanics corresponding to the canonical ensemble with a temperature related to the relative amplitudes of the random and dissipative interactions (Groot & Warren, 1997).

The time evolution of the particles in the simulation systems is governed by Newton's equation of motion

$$\frac{dr_i}{dt} = v_i, \frac{dv_i}{dt} = F_i \quad (1)$$

The masses of the particles in the simulations are set as 1. The force includes three components that are pairwise acting on each pair of particles:

$$F_i = \sum_{j \neq i} (F_{ij}^C + F_{ij}^D + F_{ij}^R) \quad (2)$$

Here, for a certain particle i , all the forces from other particles are calculated and summarized within a certain cutoff radius r_c . In all the simulations performed in this thesis, the cutoff radius used is set as $r_c = 1$. Then those three term of force components should be introduced so that we can have a detailed understanding of the interacting forces applied on each particle.

The conservative force is a soft repulsion force acting along the center lines of each pair of particles. The conservative force is given as below

$$F_{ij}^C = \begin{cases} a_{ij}(1 - r_{ij})\hat{r}_{ij} & (r_{ij} < r_c) \\ 0 & (r_{ij} \geq r_c) \end{cases} \quad (3)$$

$$r_{ij} = r_i - r_j$$

$$r_{ij} = |r_{ij}|$$

$$\hat{r}_{ij} = r_{ij}/|r_{ij}|$$

In this expression, a_{ij} is a maximum repulsion force between the pair of particles of i and j when their distance reach the maximum of cutoff radius as set by 1. $|r_{ij}|$ is the distance between the two paired particles i and j . The dissipative force can be called drag force as well.

$$F_{ij}^D = -\gamma w^D(r_{ij})(\hat{r}_{ij} \cdot v_{ij})\hat{r}_{ij} \quad (4)$$

γ is the dissipative coefficient which is set to 4.5 in our models. \hat{r}_{ij} is the unit vector between two pairwise particles and v_{ij} is the relative velocity of these two particles. The negative sign means that the dissipative force is

always opposite to the moving direction of the pairwise particles. The dissipative force impedes the relative movement between particles which results in the decrease of system kinetic energy. The loss of the kinetic energy will be compensated from the random movement caused by random force. The random force is shown as below.

$$F_{ij}^R = \sigma w^R(r_{ij}) \theta_{ij} \hat{r}_{ij} \quad (5)$$

w^D and w^R are radius-dependent weight functions vanishing for $r > r_c = 1$ and $v_{ij} = v_i - v_j$. $\theta_{ij}(t)$ is a variable that has random fluctuation. These three forces all act along the center line and conserve linear and angular momentum.

One of the two weight functions w^D and w^R can be selected arbitrarily and the other weight function is fixed by this selection.

$$w^D(r) = [w^r(r)]^2 \quad (6)$$

$$\sigma^2 = 2\gamma k_B T \quad (7)$$

For simplification, we use the expression which is similar to the conservative force.

$$w^D(r) = [w^r(r)]^2 = \begin{cases} (1-r)^2 & (r < 1) \\ 0 & (r \geq 1) \end{cases} \quad (8)$$

The time evolution of the systems is chosen by integrating the equation of motion through the velocity-Verlet algorithm (Snow, Yong, Kuksenok, &

Balazs, 2015). In the simulations performed here, r_C and $k_B T$ are chosen respectively as the characteristic length and energy scales.

$$\tau = (mr_C/k_B T)^{1/2} \quad (9)$$

γ is set to 4.5 to retain a relatively rapid equilibration of the temperature with $\Delta t = 0.02\tau$.

2.2 Atom Transfer Radical Polymerization

Due to the technological needs of application of hydrogels, we study the advanced polymer materials with well-controlled molecular structures. The synthesis of this kind of materials involves polymerization that occurs within complex, multi-component fluids. Among various polymerization methods, radical polymerization is one of the most versatile and widely applied techniques. It can generally be categorized into two types: free radical polymerization (FRP) (Yong, Kuksenok, & Balazs, 2015) and controlled/living radical polymerization (Yong, Simakova, et al., 2015). In both processes, the active chain end involves a free radical. The difference between these two polymerization processes is that the atom transfer radical polymerization does not have termination process and it has control on the conversion of polymerization (Gao, Polanowski, & Matyjaszewski, 2009). Because we have double-layered polymer hydrogels here, we need ATRP to







provide the links between first layer gel and the second layer.(Yong, Simakova, Averick, Gutierrez, & Kuksenok, n.d.)

The two samples used here are bulk polymers and double layered hydrogels (Yong, Simakova, et al., 2015). They both have a number density of 3.0. The bulk is created simply using ATRP from initiators and free monomers in the solvent of ratio of 50%. The two-layered hydrogel is formed in two steps. The first layer was successive generated with polymerization reactions. Then this polymer is put together with a solution which contains initiators, monomers and cross-linkers. The solution was introduced on top of the first layer gel. After this, we let these new components in the solution perform living copolymerization to generate the second layer gel. The living polymerization preserves species that can still react with other reactive components in the first layer gel such as active chain ends and partially reacted cross-linkers. These preserved species are able to join the successive polymerization reactions and generate chemical cross-links that link polymer chain from the two different layers. That means, these two gels from different layers can be linked covalently and create multiple layers of covalently fused gels.

The atom transfer radical polymerization (ATRP) has initiation, propagation and cross-linking of growing polymer chains (Yong, Kuksenok,

Matyjaszewski, & Balazs, 2013). Listed below are the different representation method of different type of atoms. Beads colors represent the species included in the system: initiator (magenta), monomer (blue) and cross-linker (orange). Open beads indicate that the species are unreacted or partially reacted which still have the ability to participate in the polymerization reactions. Filled beads indicate that the species are fully reacted thus they no longer have the possibility to react with other species.

Table 1 Species in ATRP

Species	Initiators	Monomers	Cross-linkers
Active			
Reacted			

Following schemes are the reactions that can be performed in the atom transfer radical polymerization.

Initiation:

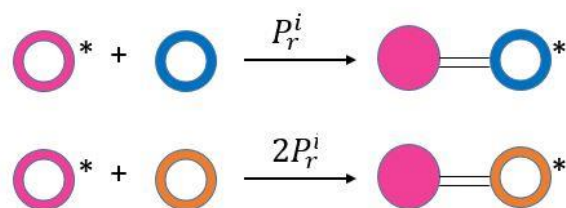


Figure 1 Initiation scheme of ATRP

Propagation:

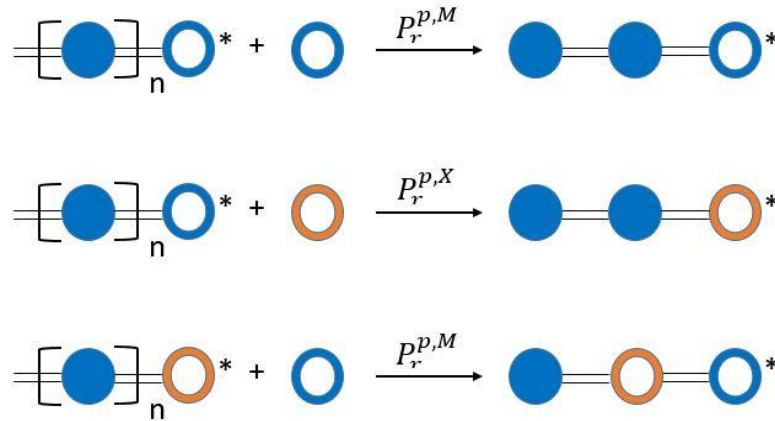


Figure 2 Propagation scheme of ATRP

Cross-linking:

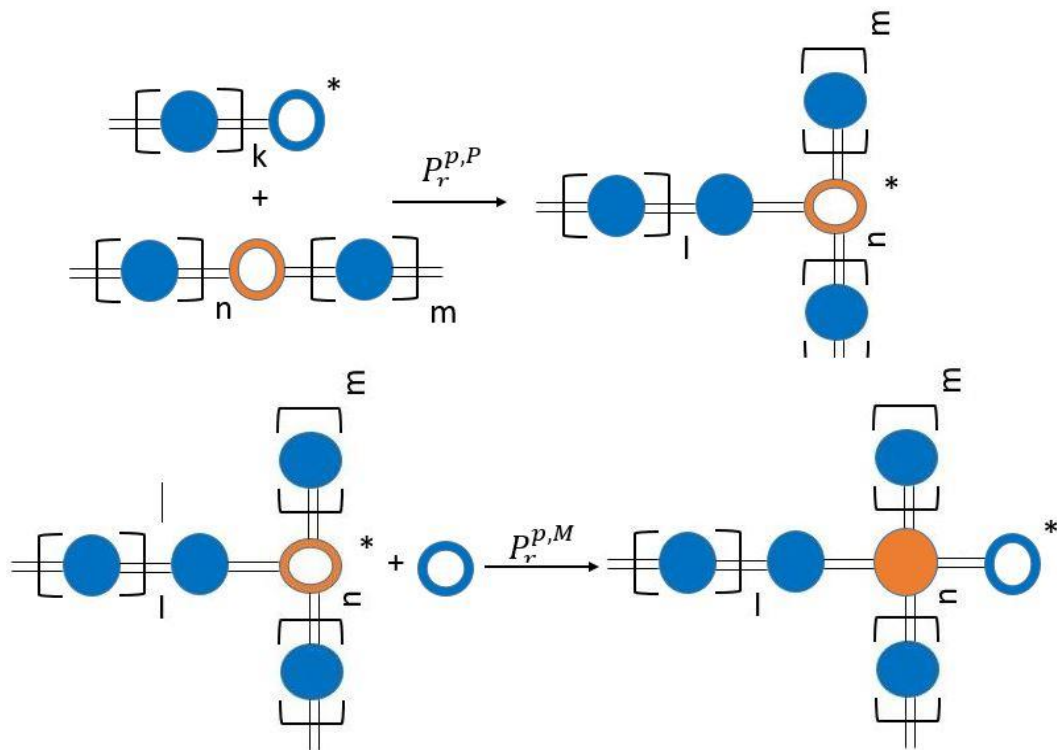


Figure 3 Cross-linking scheme of ATRP

Here for atom transfer radical polymerization, we have three kind of reactions: initiation, propagation and cross-linking. In addition to initiators and monomers, ATRP has one more type of bead called bi-functional cross-

linker. Initiators are the starters of polymerization reactions. monomers are the major components of polymer chains. Cross-linkers can react with monomers or initiators with radicals to grow chains just acting like monomers. But the most important property of cross-linkers is to form links between two different single chains to strengthen the ductility of polymer networks. Because for simple physical entanglement, it can not provide much reliable forces to keep polymer chains to entangle with each other. If the chains are linked chemically through cross-linkers, the covalent bonds will be the best agent to bind them together.

Growth of a single chain is straight-forward. As can be seen in the reaction scheme, polymer chains start with initiators. The asterisk signs represent the free radicals in the living radical polymerization. When the initiators with free radicals meet the unreacted monomers or cross-linkers with a specified cutoff radius, they will have a probability to react and form covalent bonds between them. The radical will be passed to the monomers or cross-linkers for them to perform further reactions. The initiators are the heads of every polymer chains and the free radicals are the trigger to start the reaction. After each reaction, the reacted monomers or cross-linkers will be the tail of each polymer chain, or can be called, chain ends. These chain ends with radicals will be responsible for growing longer chains if other more species

like unreacted monomers or cross-linkers are in the reaction cutoff radius and pass the probability check. A noticeable difference between initiation of monomers and cross-linkers is they have independent probabilities to react with initiators. The probability of cross-linkers to react with initiators is twice the value of monomers because the bi-functional cross-linkers have pendent functional groups grafted on them (Yong, Simakova, et al., 2015).

Propagation is a similar reaction step to the initiation except they start with monomers or cross-linkers with radicals and they have different probabilities of reactions. As introduced before, the trigger of the reactions is the radicals on the chain ends. Thus, if there are free monomers or cross-linkers roaming in the cutoff range of the living chain ends, they will have the probability to react with the chain ends and grow longer chains (Polanowski, Jeszka, Li, & Matyjaszewski, 2011). Of course the radical will always be passed to the newly formed chain ends so they can react with more species to let chains grow longer. For propagation, the probabilities of reacting with monomers and cross-linkers have to individual values which will be informed later.

Cross-linking reaction is more complex than initiation and propagation. But still, the pivotal part is the radicals affiliated to the chain ends. Because of the pendent functional groups on the cross-linkers, every cross-linker can react at most four times and have four covalent bonds attached to it. There

are two reactions in the cross-linking process. One is the chain ends reacting with radicals reacting with partially reacted cross-linkers and the other is the partially reacted cross-linkers in the polymer network reacting with a new free monomer to generate a new chain grafted on the cross-linker thus the new chain will provide more toughness to the polymer network. But since one cross-linker can have at most four covalent bonds in the three-dimensional system, the cross-linker will lose the ability to generate more chains as long as it already has four chains grafted on it. Once it starts to cross-link, the newly grafted chains can either propagate or cross-link with regard to the probabilities checking within the cutoff radius.

3. Fracture Model

3.1 Harmonic Bond

We want to explore the mesoscopic mechanical response of the chemically cross-linked polymeric system with 50 percent of solvent. Thus a bond breaking model have to be introduced into the simulation. Before eliciting the bond breaking model, we want to give a brief explanation of the covalent bond used in the simulation. The polymer chain we used in the system is basically a bead-spring model as introduced before. Therefore, we choose harmonic bond which is a spring-like type of chemical bond with a bond potential of (Doerr & Taylor, 1994)

$$E = \frac{1}{2}K(r - r_0)^2 \quad (10)$$

where r_0 is the equilibrium bond distance and K is the spring constant of the covalent carbon-carbon bond. Specifically, the spring constant is set to 128 in all the simulations. And the equilibrium bond distance is set to 0.5.

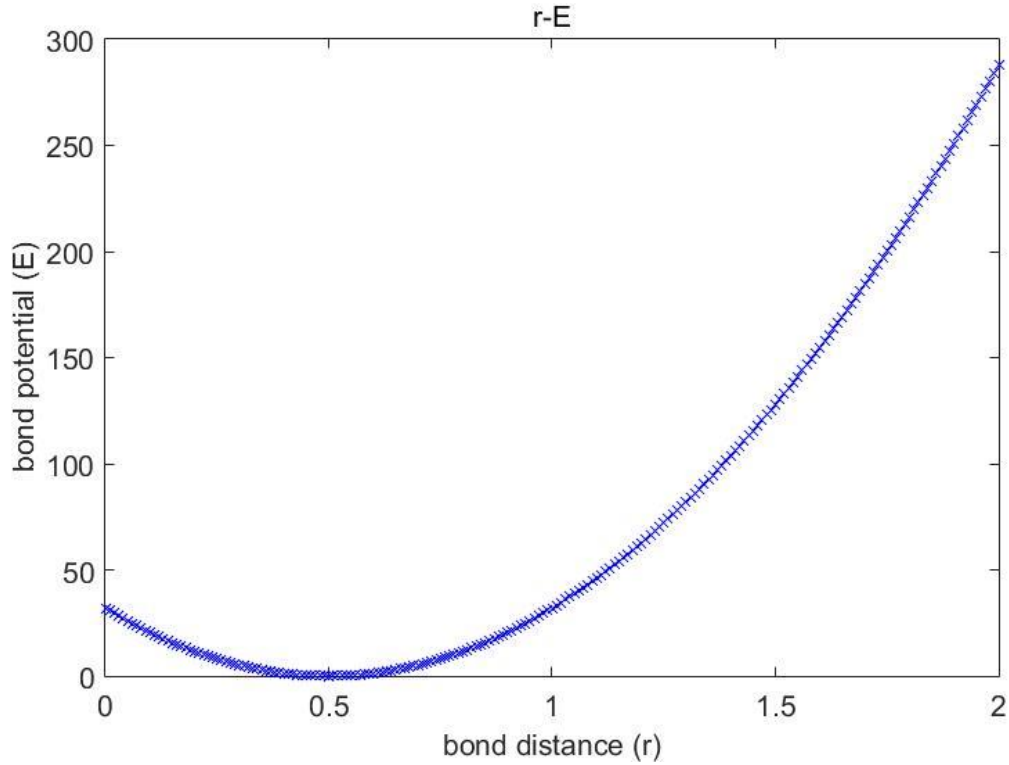


Figure 4 Potential energy for harmonic bonds

Bond potential is the second order to the bond distance. But since the polymer network simulated here is amorphous polymer hydrogels, the stress corresponding to the strain of the whole sample does not act like this curve. This will be clarified later in the result section. Also we do not use big value of bond constant K for the harmonic bonds in our systems because higher bond constant leads to significant increase of bond potential when bonds are elongated. And thus, when we apply the bond breaking to the system, the dramatic change in system energy will lead to bad dynamics.

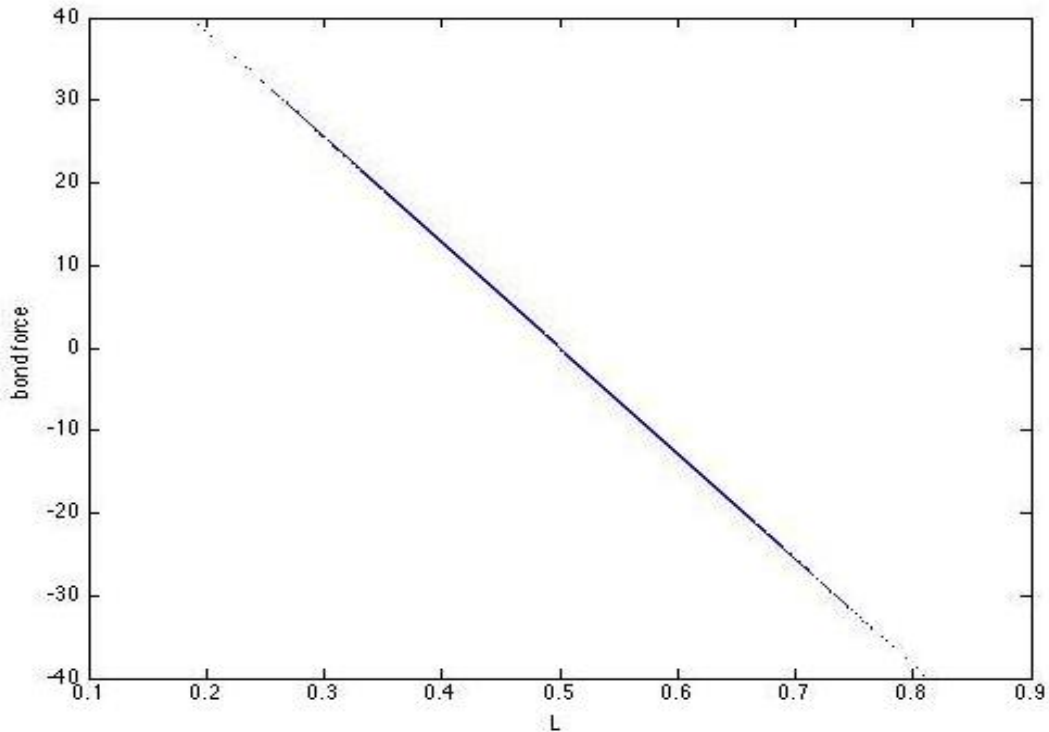


Figure 5 Bond force for harmonic bonds

Bond force is also monitored to see whether the bond act normally when it is under uniaxial stretch. The bond does not have any internal force when it is at its equilibrium length of 0.5 as assigned. The value of bond force is positive when it is under compression and negative when it is elongated.

3.2 Bond breaking model

Like the model of polymerization, cutoff radius is used as well in bond breaking part. But the different part is that the focused element is bond instead of atoms. Once the C-C bond is stretched and longer than its equilibrium length, we check its eligibility and probability for breaking. While stretching the simulation box with a constant strain rate, every bonds are looped and assigned a

probability based on their length, energy, characteristic vibration frequency and total external forces with regard to the equation below (Iyer, Yashin, Hamer, et al., 2014).

$$P_b = v * \exp^{-U_0/k_bT + F_{ext}\gamma_0} \quad (11)$$

The first term of the exponential is the break rate without any external force

$$P_b = v * \exp^{-U_0/k_bT} \quad (12)$$

Here, U_0 is the basic bond energy. $140 \text{ } k_bT$ is used as the energy of carbon-carbon bonds. v is the characteristic frequency of bonds which is usually $2.0 \times 10^{13} \text{ } s^{-1}$ (Iyer, Yashin, & Balazs, 2014). The flow chart of bond breaking process is as shown below.

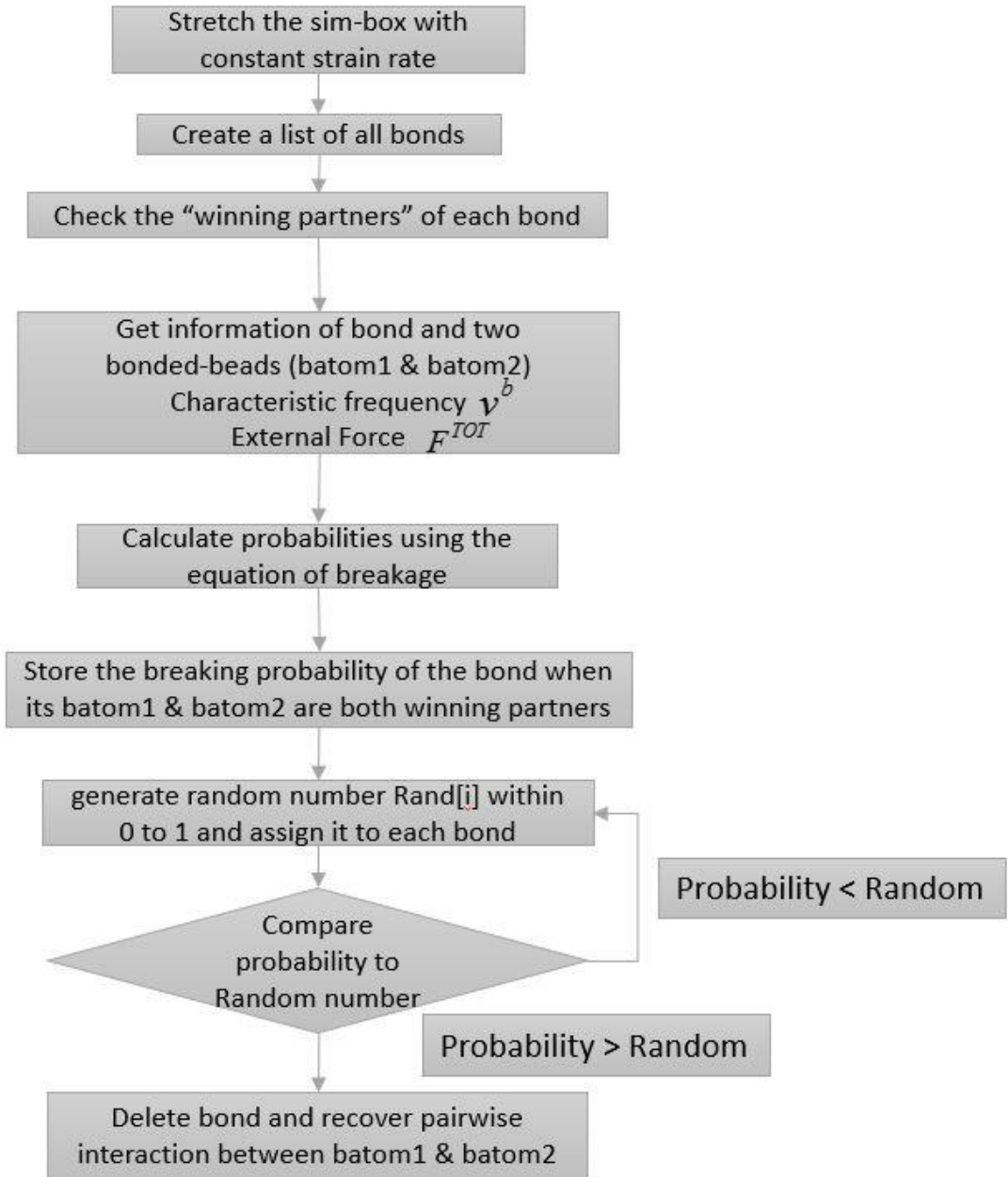


Figure 6 Flow chart of bond breaking

First the uniaxial tensile strain is applied to the simulation box at a constant strain rate. Then we create a list of the information of all the bonds in the simulation box. After this we have a selection of all the bound atoms called “winning partner”. For a pair of atoms i and j on the two ends of a single

bond k . We read all the bond length information attached on i and j . If bond k is the longest bond attached on i and j , we call this bond the winning bond and the two atoms are the winning partners. Then this winning bond is eligible to break. We go through all the bonds in the list created previously and select all the winning bonds to generate a new list of them. Then we track all the necessary information of those bonds. The information we need is the total external force acting on each winning bond, as by saying, the net force along the direction of the center-to-center line of two winning partners. For bond k , we read the force information of atom i and j if the bond is eligible to break. We have six force components $F_x^i, F_y^i, F_z^i, F_x^j, F_y^j, F_z^j$. The forces from the winning partners already have the bond force included. And the coordinates of these two atoms to get the center-to-center line $C_x^i, C_y^i, C_z^i, C_x^j, C_y^j, C_z^j$.

$$F_{ext} = F_2 - F_1$$

$$F_1 = \frac{F_x^i(C_x^i - C_x^j) + F_y^i(C_y^i - C_y^j) + F_z^i(C_z^i - C_z^j)}{r_b} \quad (13)$$

$$F_2 = \frac{F_x^j(C_x^i - C_x^j) + F_y^j(C_y^i - C_y^j) + F_z^j(C_z^i - C_z^j)}{r_b} \quad (14)$$

Then we decompose these six force components to the direction of center-to-center line which is actually the direction of the bond and add all the decomposition forces up to get the total external force acting on the bond. This total external force is not just the simple bond force because bond force is an internal force that correspond to the bond length with regard to the spring constant of the bond potential. But we also have DPD force on the bound atoms from other polymer chains and solvent. Then we calculate the probability of bond breaking for each winning bond and create a list to store the probabilities using the previously introduced expression.

4. Equilibration at Constant Pressure

Most experiments studies in condensed matter are conducted at constant temperature and constant pressure. Since the simulating objects are dynamic systems, an equilibration method needs to be applied in the simulation (Martyna, Tobias, & Klein, 1994). And because of the incompressibility of hydrogel, we have to get an approximate value of hydrostatic pressure to make sure the volume of the system will not change although the volume will have small fluctuation when we apply the ensemble settings to it (Gao et al., 2009). For most of the simulations done for polymerization, constant volume and constant temperature are used to reach the equilibrium of system. But for the system that contains bond breakage and thus the sudden change in system energy due to the loss of bond energy, NVT and NPT can lead to magnificent difference in the system structure (Trofimov, Nies, & Michels, 2005).

Here we choose the Andersen barostat for pressure control and we do not need to add another thermostat because the temperature of the system has already been controlled in DPD by the interplay of dissipative and random forces (Jakobsen, 2005).

5. Results

We want to observe the bond breaking behavior of polymeric systems and analyze the influence that be done to the system by this fracture. We use this mesoscale modeling to predict the properties of materials which are determined by the conformation and dynamics. Here, all the models we used have the same number density of $\rho = 3$ which represents the density of water in the systems. The repulsion parameter for polymer-polymer, solvent-solvent, polymer-solvent are $a_{ij} = 25$. Specifically, since the two-layered hydrogels have air layers on the top and bottom of the simulation box for preventing two interfaces. In order to prevent the particles from being shot out of the box due to high velocity after breakage, the repulsion between air and other particles is set to $a_{ij} = 120$. The dissipative coefficient is set to $\gamma = 4.5$ in order to get a relatively rapid equilibration of the system temperature.

5.1 Simplified Single-Chain System

Table 2 Parameters for single-chain systems

Box dimension	$6 \times 6 \times 10$
Number density (ρ)	3.0
Repulsion parameter (a_{ij})	25
Dissipative coefficient (γ)	4.5
Number of polymer particles	20
Number of solvent particles	1060

First, we want to focus on the basic behavior of bond breakage in a simplified single-chain system with 20 atoms. This single chain is put into a $6 \times 6 \times 10$ simulation box with periodic boundary condition and 1060 atoms of solvent beads are put into the box as well to make sure the number density of the system to be $\rho = 3$. Then we set the ensemble of external pressure to be 23.75 from a pure solvent system with the same number density and other parameters to keep the volume constant and let the sample relax to its minimum residual stress. We can see that the system only spends a short time period to reach the expected pressure. Below is the expression of pressure of the simulating system.

$$P = \frac{Nk_B T}{V} + \frac{\sum_i^N r_i f_i}{dV} \quad (15)$$

N is the number of atoms in the system, k_B is the Boltzmann Constant, T is the temperature, V is the volume of the system, d is the dimensionality (3 for 3D system here). Second term is the virial term. In the virial term, r_i is the position of atom i and f_i is the force acting on the atom which is the combination of pairwise interaction and bond force.

Following is the calculation of six components of pressure.

$$P_{I,J} = \frac{\sum_k^N m_k v_{kI} v_{kJ}}{V} + \frac{\sum_k^N r_{kI} f_{kJ}}{V} \quad (16)$$

The six components are xx, yy, zz, xy, xz, yz and I, J stand for x, y, z. This equation is similar to the first equation. The difference of this equation comparing to the equation above is that the first term of this equation uses the components of the kinetic energy tensor and the second term is from the virial tensor (Thompson, Plimpton, & Mattson, 2009).

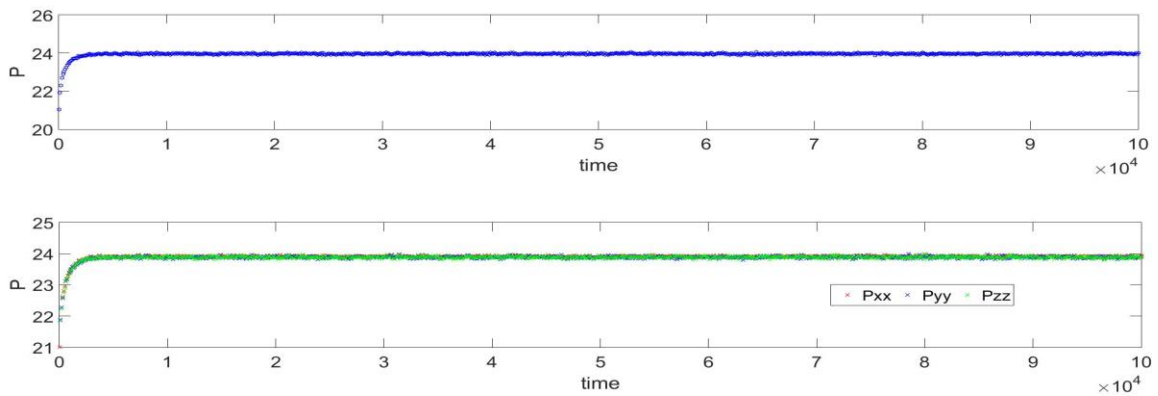


Figure 7 Pressure profile of pure solvent sample

The origin state and the equilibrium state of the sample are shown as below.

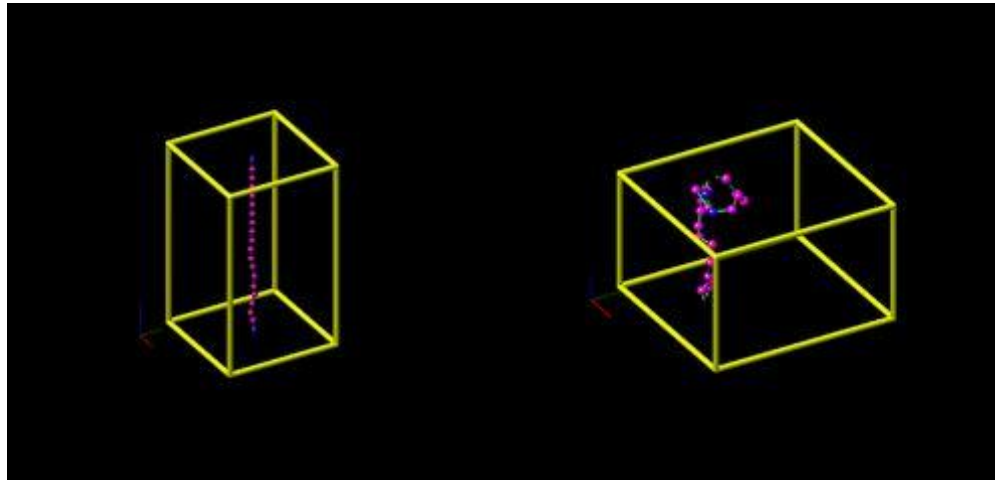


Figure 8 Origin and final structure of single-chain model

Then we start to deform this sample and let the bond breaking work during the stretch at a constant strain of 0.0001 per 10 time steps. After running 1,000,000 time steps, the simulation box is stretched to double of its equilibrated original length. During the NPT ensemble of 100,000 time steps, because the sample is not pure solvent but solvent with polymer chain and polymer chain tends to coil to its equilibrium state (Lorenz et al., 2004). the pressure in the z-direction is lower than the other two directions. At the equilibrium state, the simulation box is flatter than a cubic box under isotropic pressure. And after the elongation and bond breakage. The volume, pressure and temperature profile are shown below.

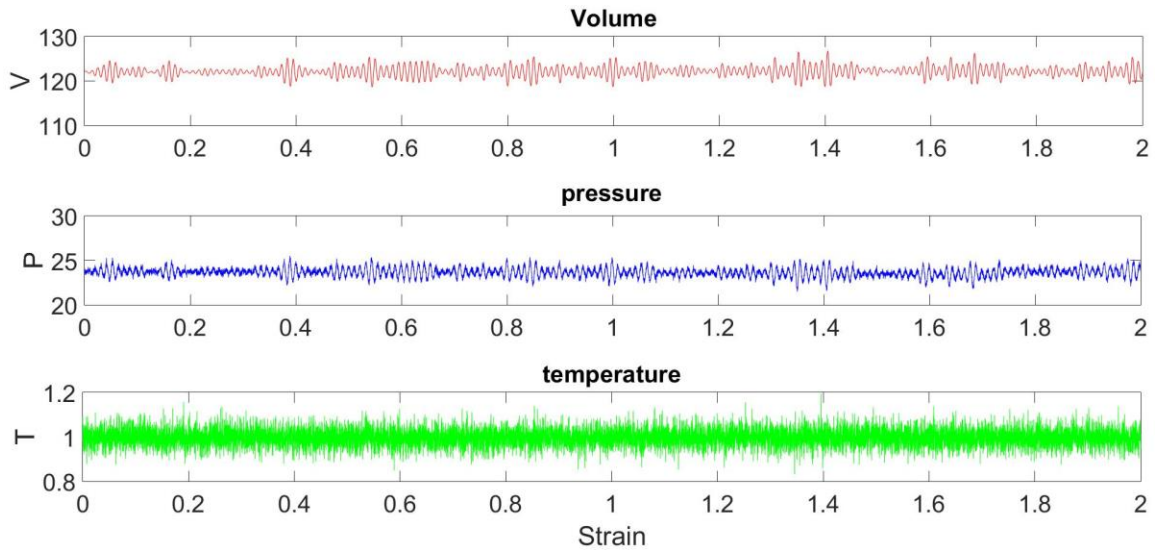


Figure 9 Volume, pressure, temperature profile

Since this is just a very small system with only one chain in it. And this one chain will bounce back like a rubber after one bond is broken, the volume, pressure and temperature will not change but only have regular oscillation due to the NPT ensemble. The volume stays at around 359 like the original volume before strain is applied and after constant pressure equilibration, so do the pressure and the temperature.

In order to observe the bounce back of the chain after breakage, we use the exact same parameters and random seeds to run again the simulation and plot the snapshots more frequently.

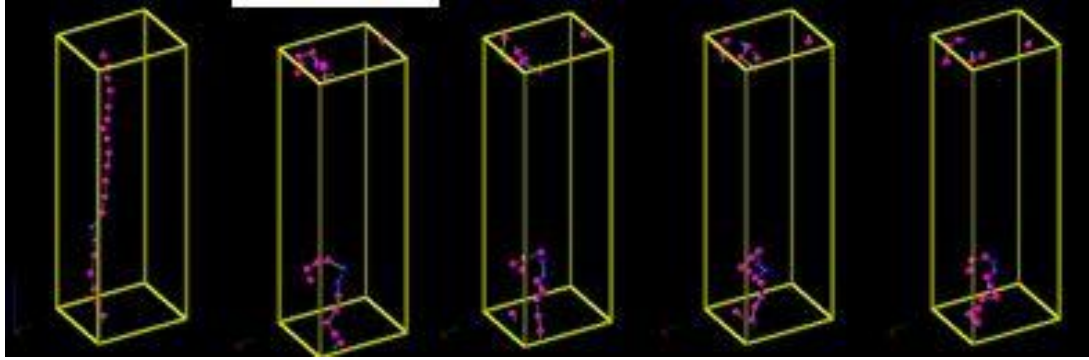


Figure 10 Snapshots of continuous movement of broken chain

As can be seen in Figure 10, the chain will not stand straight after one bond breaks because for the bond breaking system, the bond force will be instantly taken out when it is broken. But before it breaks, it will experience a relatively large external stretching force to help it reach the probability and length to break. After the bond breaks, the newly created two chain ends will have two atoms with high force on them to drag them back like a spring (Sheka & Popova, 2011). But at last, these two ends will stay at the top and bottom boundaries, not going further. Because the rest of the bonds will be compressed due to the bounce back and provide repulsion to push the chain ends back. And also the soft repulsion from those solvent beads will also contribute to the resistance of further movement.

Recall the bond breaking model expression

$$P_b = v * \exp^{-U_0/k_bT + F_{ext}\gamma_0}$$

Since v is the bond vibration frequency set as $2.0 \times 10^{13} s^{-1}$ here for carbon-carbon bond. It is a natural property of chemical bonds which cannot be

tuned. U_0 is the basic bond energy fixed as $140 k_b T$. F_{ext} is the variable that depends on the dynamics of the system. Then the only one parameter that we can tune is the bond sensitivity γ_0 .

I plot the probability curve with regard to the external forces to see how the bond will break under a rising force using different bond sensitivities.

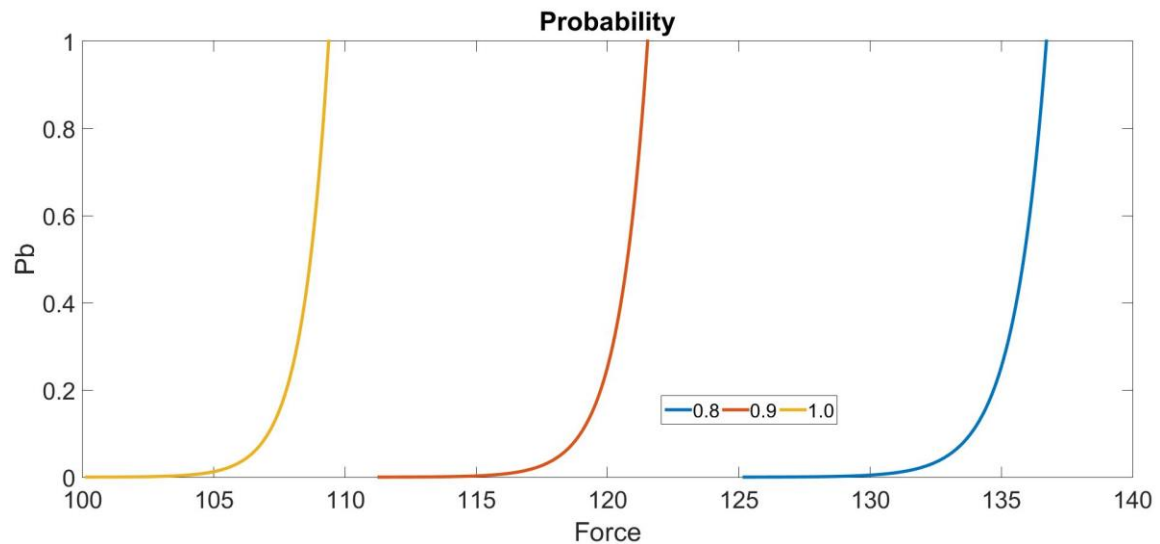


Figure 11 Probability curve

As can be seen in Figure 11, for the various bond sensitivity chosen, the probability curves all have a significant increase after a certain external force is reached because the exponential of the expression. Recall the bond potential formula of harmonic bonds and the internal bond force under elongation, the component that determines the actual external force for bond to break is the spring constant K of the harmonic bond. Larger value of bond sensitivity makes the bond breaks at a lower external force. That means,

with the same bond constant K , the bond with larger sensitivity will break with less elongation.

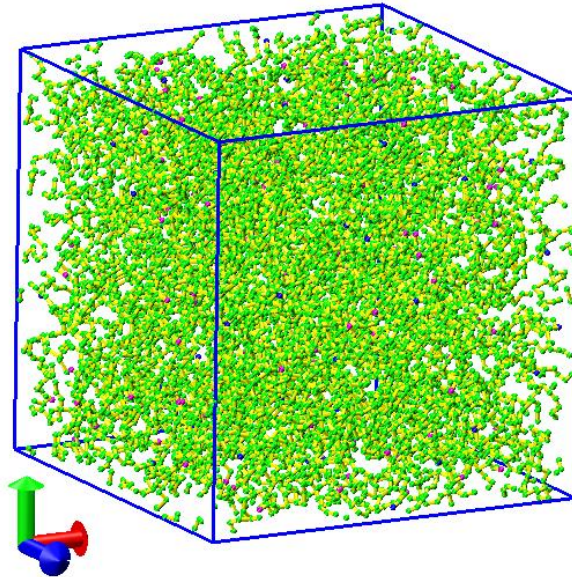


Figure 12 Bulk polymerization at conversion of 90%

5.2 ATRP Bulk Polymers without Cross-links

Table 3 Parameters for bulk polymers formed using ATRP

Box dimension	20×20×20
Number density (ρ)	3.0
Repulsion parameter ($a_{all-all}$)	25
Dissipative coefficient (γ)	4.5
Number of polymer particles	12000
Number of solvent particles	12000
$[Ini]_0/[M]_0$	1/75

The bulk polymer is simulated in a 20*20*20 box with 24,000 atoms in it including 50% of solvent. Thus the number density is also 3.0. So we use the same external pressure constant as the pure solvent model. As explained before, different colors are assigned to different type of species:

- Initiators (heads of chains) are in the color of magenta
- Fully reacted monomers are in the color of green
- Active chain ends (tails) are in the color of blue
- Covalent bonds in the chains are in the color of yellow

As can be seen in the configuration of polymer, the chains' growth has not stopped yet because we can still observe some active chain ends in the color

of blue. Another thing we can observe here is that the chains grow long and entangle with each other in a complex structure.

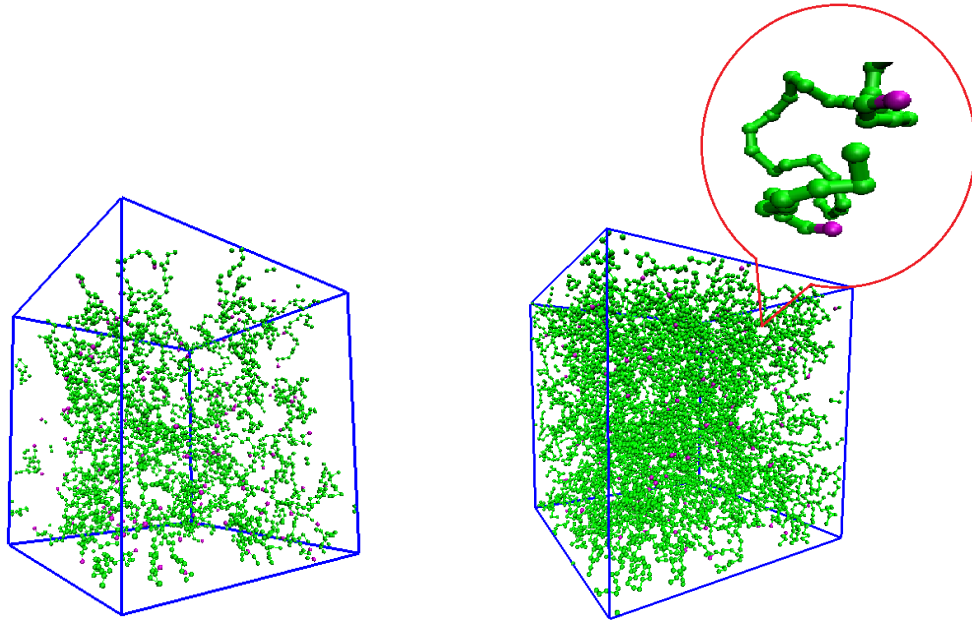


Figure 13 Bulk polymer at conversion of 15% and 50% Bulk polymer under different conversion are as shown in Figure 13. The 50% snapshot is much denser than the 15% one. And from the zoomed picture we can see the polymer chains and colors clearly. The bonds are colored regard to the type of atoms respectively. The sample is then polymerized till its conversion of 95% to make sure it has high molecular weight and consume most of the monomers (Termonia, Meakin, & Smith, 1985).

After the first equilibrium, we apply a slow strain on the z-direction of the sample. The strain rate is 0.0005 per 100 time steps. The sample will be elongated to 10 times of its original length within 1,000,000 time steps. And at the same time, break bonds per 200 time steps with two different bond

sensitivities of 1.0 and 0.9. We have three simulations for bulk polymer. First one is stretch without bond breaking. Second one is stretch with bond breaking and sensitivity of 1.0. Third one is stretch with bond breaking and sensitivity of 0.9. We check the system properties then.

5.2.1 Bulk Polymers Under Stretch and No Bond Breakage

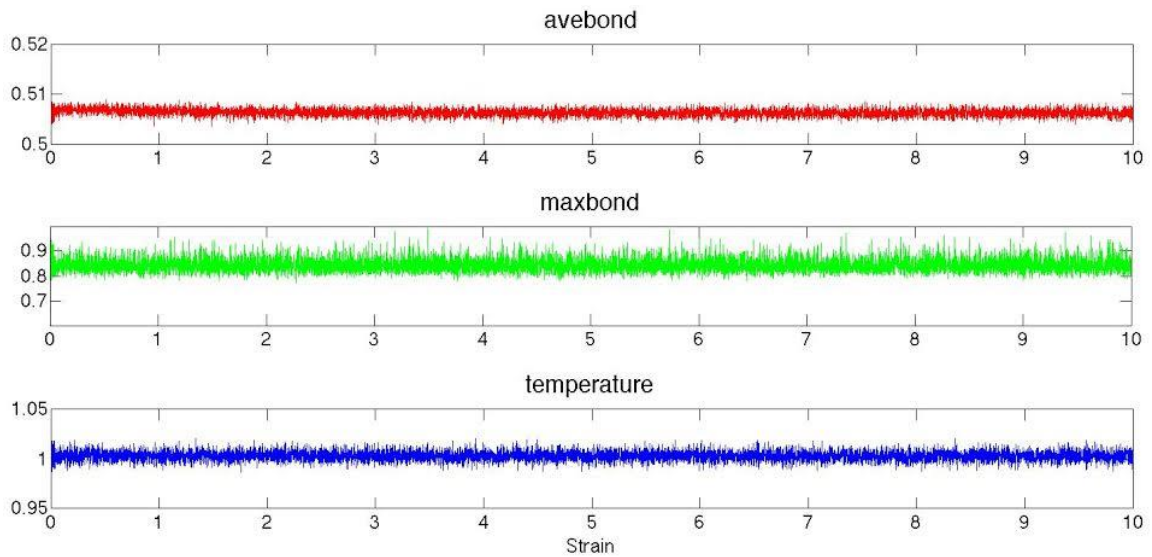


Figure 14 Average bond length, maximum bond length and temperature profile. The average bond length, though it has little fluctuation due to the dynamics, stay at the level about 0.507. Because of the physical entanglement of the system, the average bond length will not reach the equilibrium length set as 0.5. But the interesting point is that even though the sample is stretched to tenth its original length, the average and maximum bond length does not change. That's because lack of cross-linkers to strengthen the polymer network, those independent chains have the freedom to slip and get rid of the only resistance, physical entanglement.

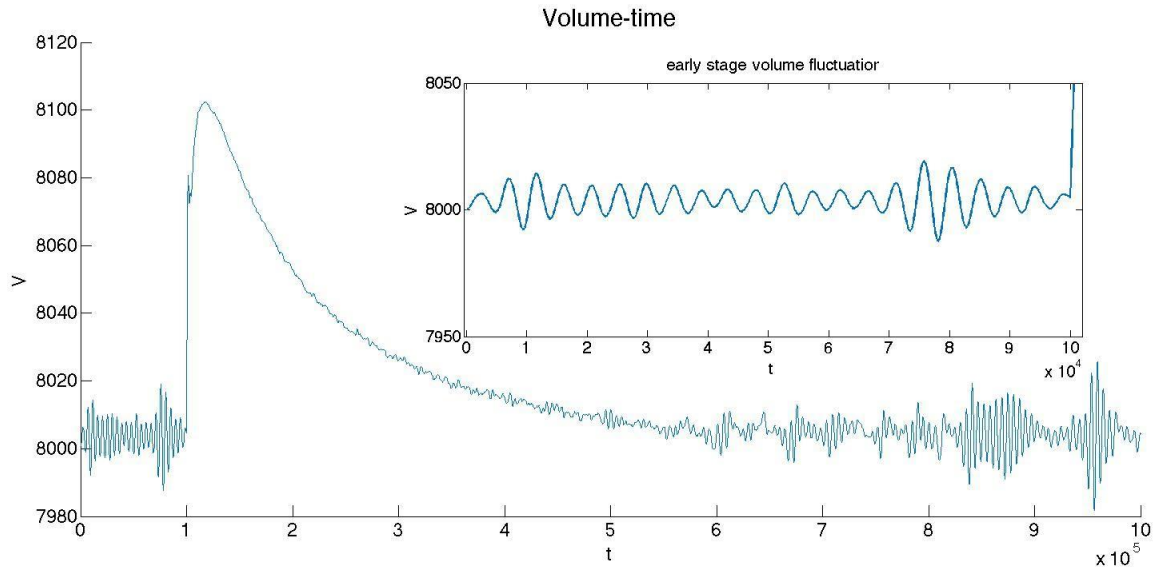


Figure 15 Volume change under stretch

Figure 14 is the volume corresponding to the time. The first 100,000 steps are the early stage of NPT equilibration without stretch. There is a significant upward curvature to 8,100 when the sample start to be stretched and gradually recover to its original volume. We cannot apply constant pressure on the z-axis because the deformation is applied to it. Thus we fix isotropic barostat on the x and y direction. But still, although the deformation and the equilibration are processed simultaneously, it needs time for the x and y directions to correspond to the deformation. That is why the volume will rise at first. The value is not big but still noticeable.

5.2.2 Bulk Polymers Under Stretch and Bond Breakage

We have studied the mechanical response of a bulk polymer without fracture. Now we turn our sight to the fracture part of the same sample. First we try to use a bond sensitivity of 1.0. As seen from Figure 17, the bonds start to

break at the very beginning of deformation and the speed of breaking does not slow down. Under this circumstance, sensitivity of 1.0 is too large. It even let bonds break at very small deformation. The average bond length decreases because a large amount of long bonds are broken and they break uniformly. This does not meet the requirement of our simulation. So we decide to tune the sensitivity to 0.9 to get a more reasonable fracture behavior.

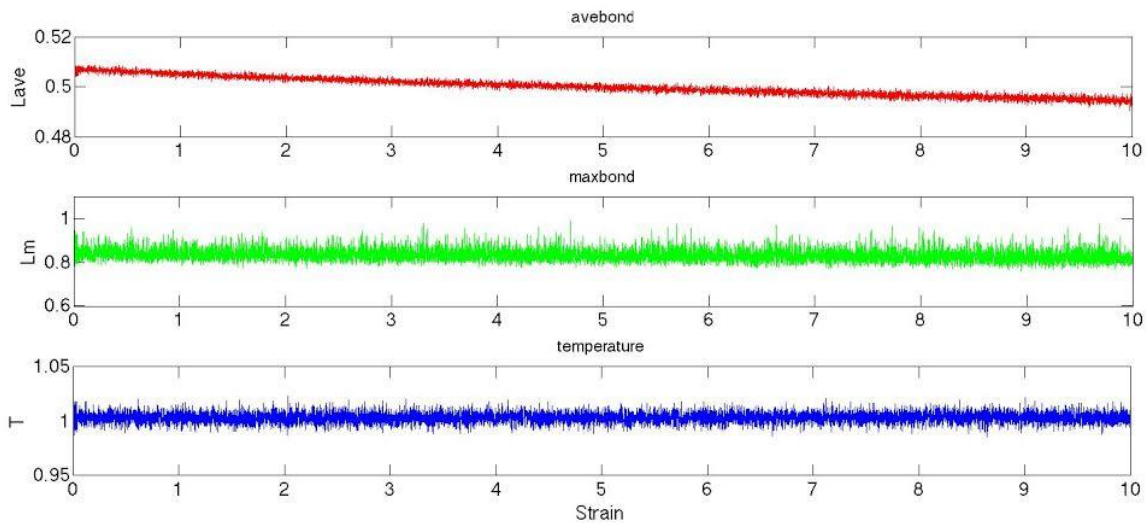


Figure 16 Average, maximum bond length and temperature curve with 1.0 sensitivity.

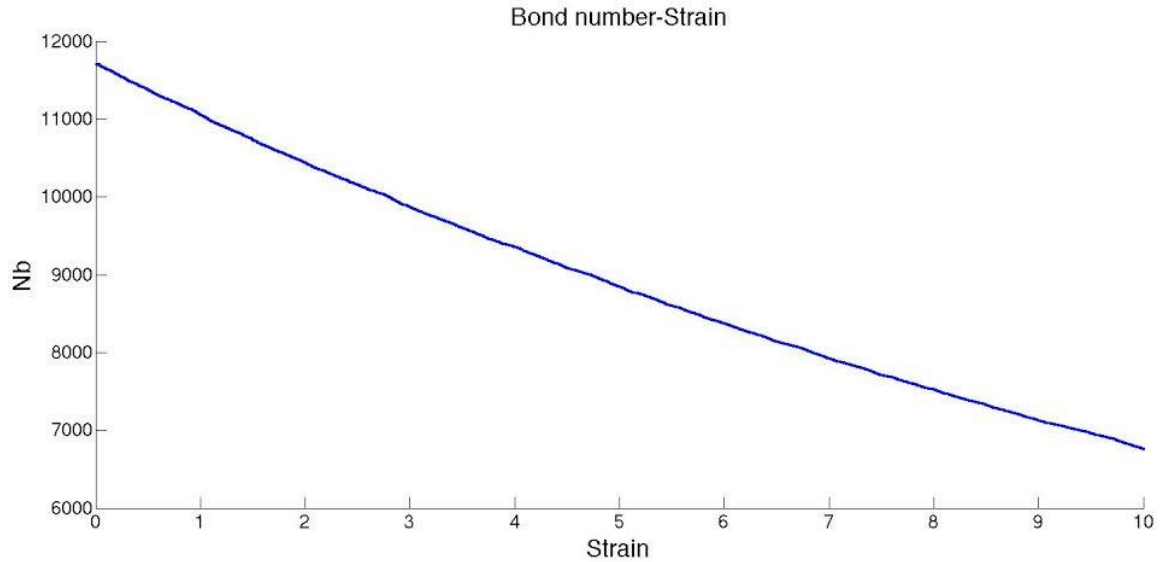


Figure 17 Bond number profile of 1.0 sensitivity

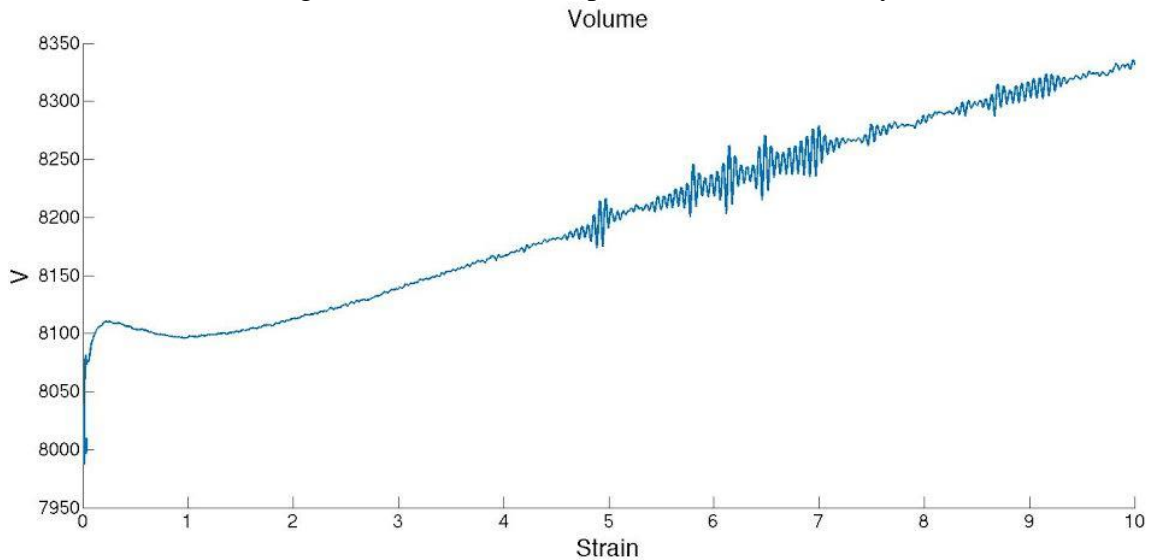


Figure 18 Volume profile of sample with 1.0 sensitivity

The following figures are the profiles of a sample with 0.9 sensitivity. We can see the breakage no longer happen frequently at the beginning of deformation. Although the residual long bonds after equilibration make it possible to break a small amount of bonds at early stage of the simulation.

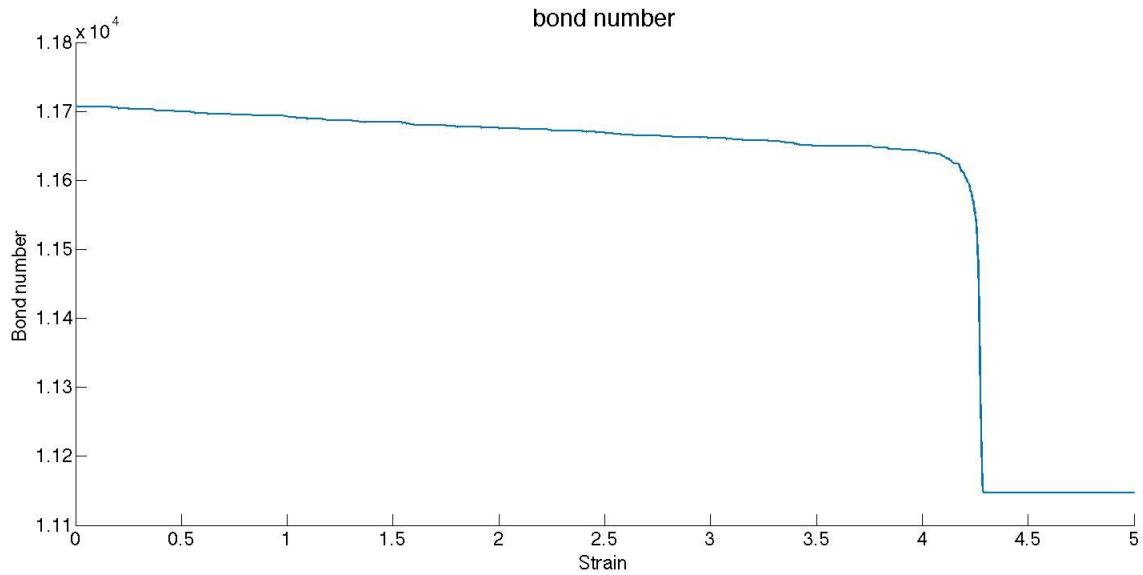


Figure 19 Bond number of bulk with 0.9 sensitivity

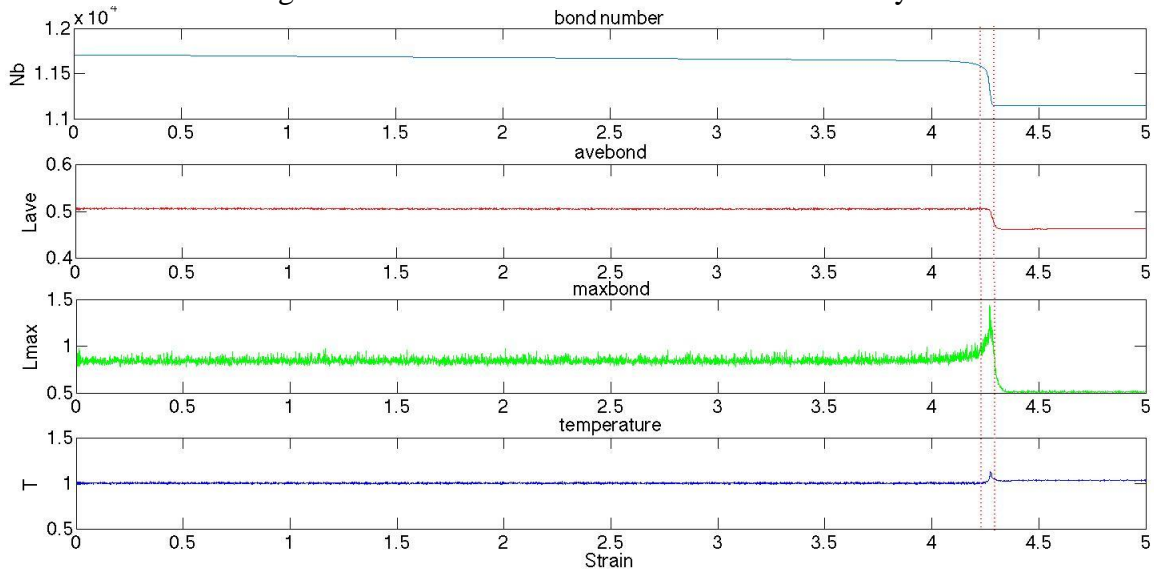


Figure 20 Bond number, average, maximum bond length and temperature profile. In Figure 20, It is noticeable that when the large amount of bonds breaks, the average bond length decreases due to the breakage of long bonds and the temperature at this point has a small peak due to the big value of chain ends velocity created by the required force of bond breaking. The maximal bond length increase from around 0.8 to roughly 1.5 during the bond breaking

period and fall back to almost 0.5 which is the equilibrium length of harmonic bonds. We want to investigate the reason that the maximum bond length goes rapidly right before the bonds break. So we take a look at the summarized pairwise energy and bond energy of the system.

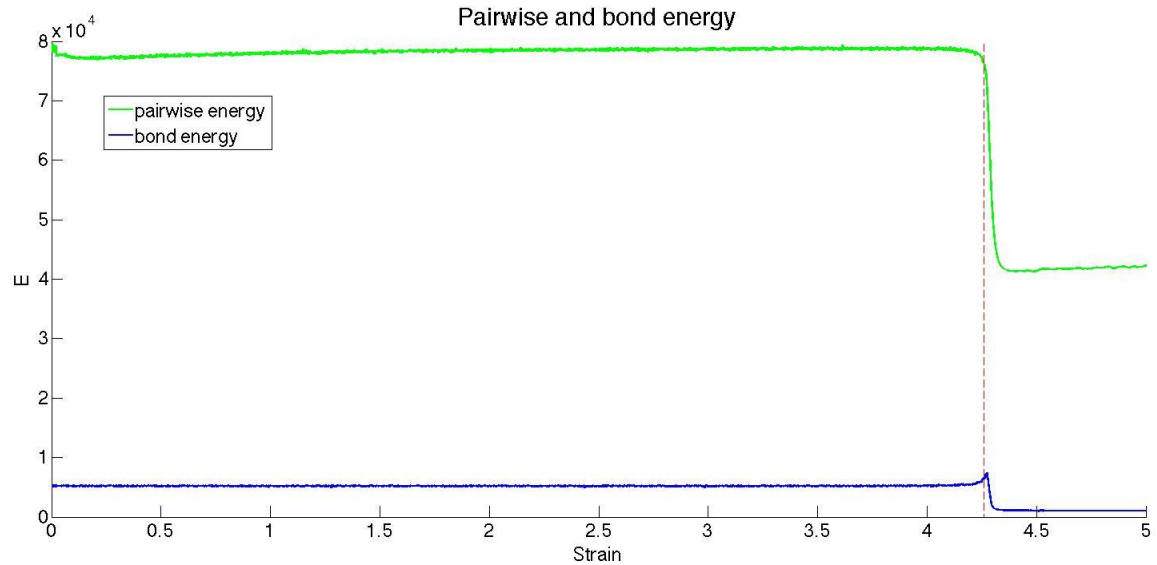


Figure 21 Pairwise and bond energy of the system

Figure 21 shows the pairwise and bond energy of the system, pairwise energy is in green line and bond energy is in blue line. We can see the bond energy drop down near to 0 because under equilibrium state, most of the bonds should reach the equilibrium length and the average bond length in Figure 20 is almost 0.5. We see a significant drop in the pairwise energy. As discussed previously in this thesis, the intense movement of free chain ends created by bond breakage leads to high value of dissipative force opposite to the relative velocity to suppress the relative movement. This process will

significantly reduce the system energy while the number density of the system remains the same. The bead-spring model of our bond breakage create high velocity chain ends which can lead to few extremely long bonds during the bond breaking and make the system temperature increase thusly.

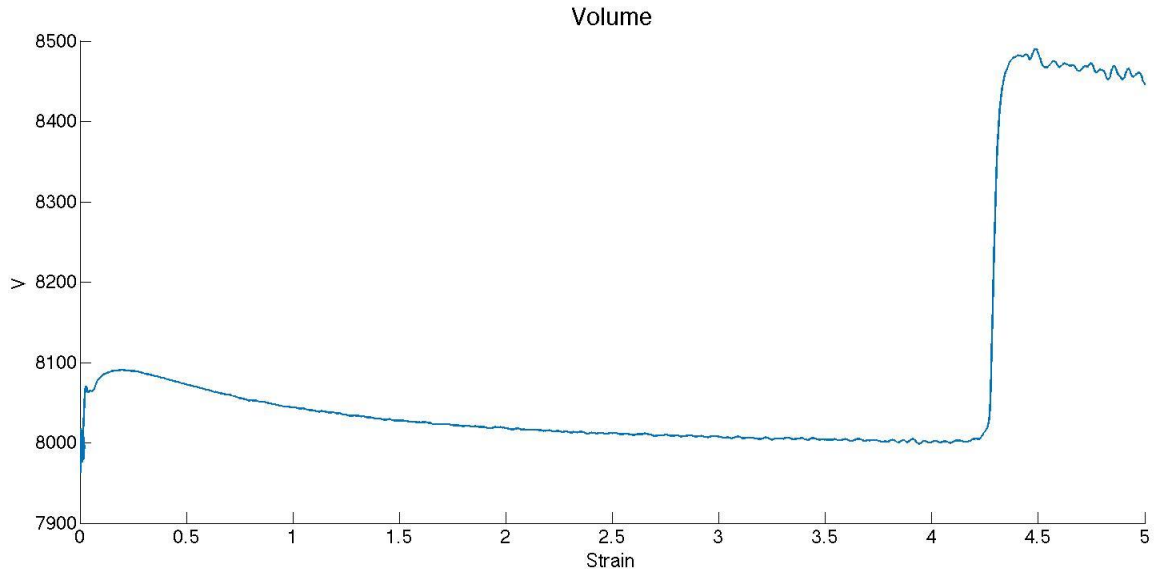


Figure 21 Volume profile of sample with 0.9 sensitivity.

Figure 21 is the volume corresponding to the bond breakage behavior. The volume of bulk polymer will increase rapidly when an obvious quantity of bonds breaks. Recall how pressure is calculated for the system

$$P = \frac{Nk_B T}{V} + \frac{\sum_i^N r_i f_i}{dV}$$

The mechanism of bond breakage is completed by turning off the bond interaction and turning on the pairwise interaction between i and j . At certain strain, we lose a noticeable amount of bonds which leads to an instant reduction in virial term with constant external P and N . As can be seen in

Figure 5, the bond force is 0 at the bond length of 0.5 and the value goes negative when the bond is under stretch. The significant loss of negative value of bond force in the virial term of the system leads to the pressure increasing of the system. But the simulation is under constant pressure ensemble. Therefore, the volume of the simulation box will expand to keep the pressure consistent with the set value of pressure.

5.2 Two-Layered Composite Hydrogels with Cross-links

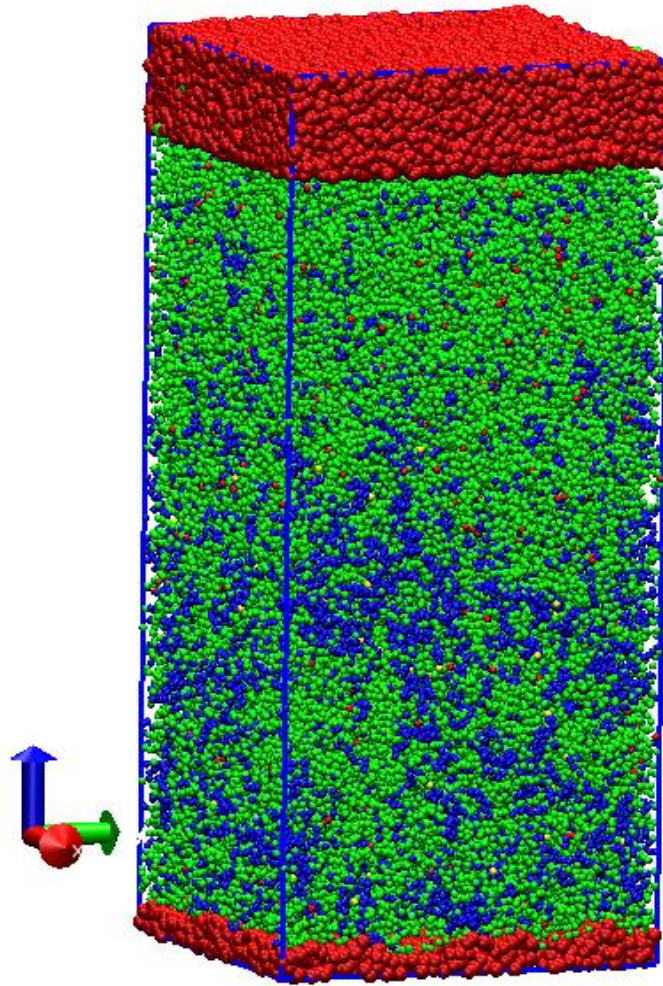


Figure 22 Double-layered hydrogel.

The two-layered hydrogel formed via ATRP is shown as Figure 22. At first we form a single layer of ATRP hydrogel which is represent using blue color in the figure. Then we put the first layer into a solution with initiators, monomers and cross-linker. The newly added species can also flow into the first layer through the interface to react with the active chain ends or partially-reacted cross-linkers so that these two layers will have convection flows and make the gel even stronger. Since there are cross-linking reactions in the formation of two-layer gel, the denser polymeric network of this sample is the more ductile it is than the bulk polymer. There are at most four bonds that can be formed on a single cross-linker (Yong, Simakova, et al., 2015). Thus the contract of polymer chains after bond breakage is faster than those in the bulk. That means, the polymer network could provide even larger retracting force after one bond breaks. As usual, we first take a look at the properties during NPT equilibration before start the deformation. Same to the single-chain system, we use the hydrostatic pressure got from NVT pure solvent system.

Table 4 Parameters for two-layered hydrogels with cross-linking

Box dimension	30×30×70
Number density (ρ)	3.0
Repulsion parameter ($a_{solv-polv}$)	25
Repulsion parameter ($a_{solv-solv}$)	25

Repulsion parameter ($a_{poly-poly}$)	25
Repulsion parameter ($a_{air-aer}$)	120
Dissipative coefficient (γ)	4.5
Number of polymer particles	94500
Number of solvent particles	94500
$[Ini]_0/[X]_0/[M]_0$	1/5/75

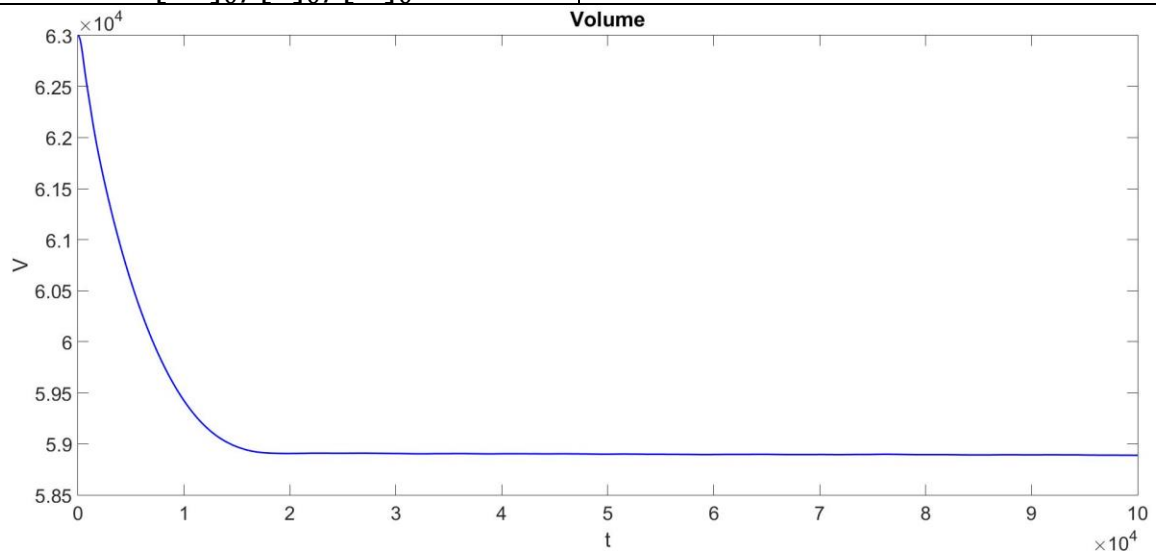


Figure 23 Volume profile of NPT equilibrium.

The equilibration takes effects in a short period of time as well. Since there are cross-linked polymer networks in the sample. The polymeric system with fifty percent of solvent shrink a certain ratio from 63,000 to roughly 58,800.

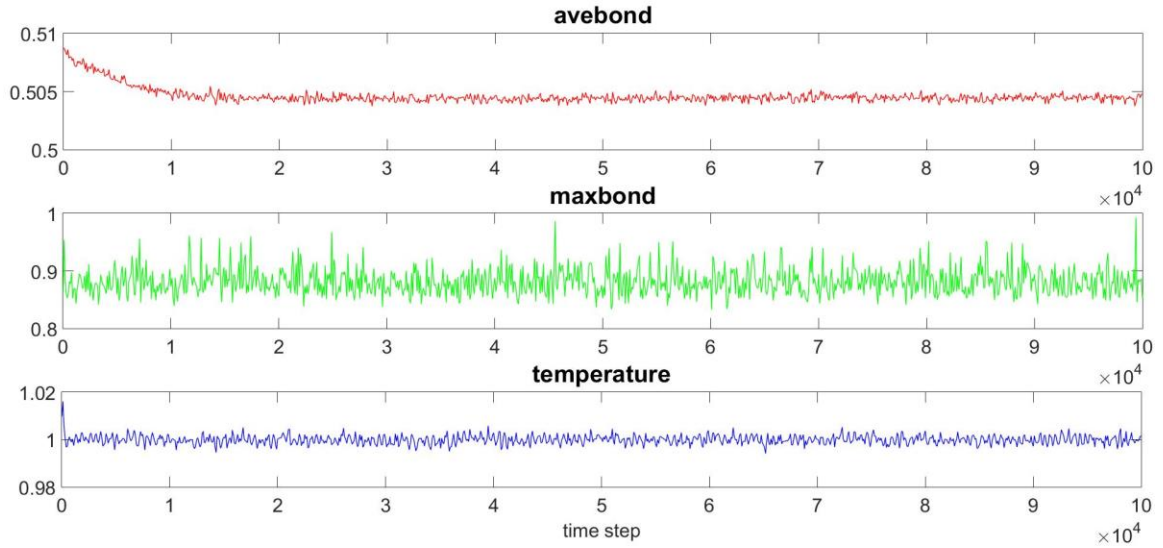


Figure 24 Bond and temperature information of NPT.

During the relaxation of the system, average bond length decreases but still does not reach the equilibrium length. Since this is a two-layered hydrogel, we want to predict whether the ductility and stiffness of the interface are better than a simple generated gel or not. As mentioned previously, we use 0.9 of bond sensitivity for the hydrogel system. The strain rate used for this case is 0.0005 per 100 time steps. The two-layered sample is deformed to 400% strain. Since we want to observe more obvious fracture phenomenon during deformation, we only spend 400,000 time steps to let it reach the expected strain. Therefore, we can check the material property under stretch through checking the density profile.

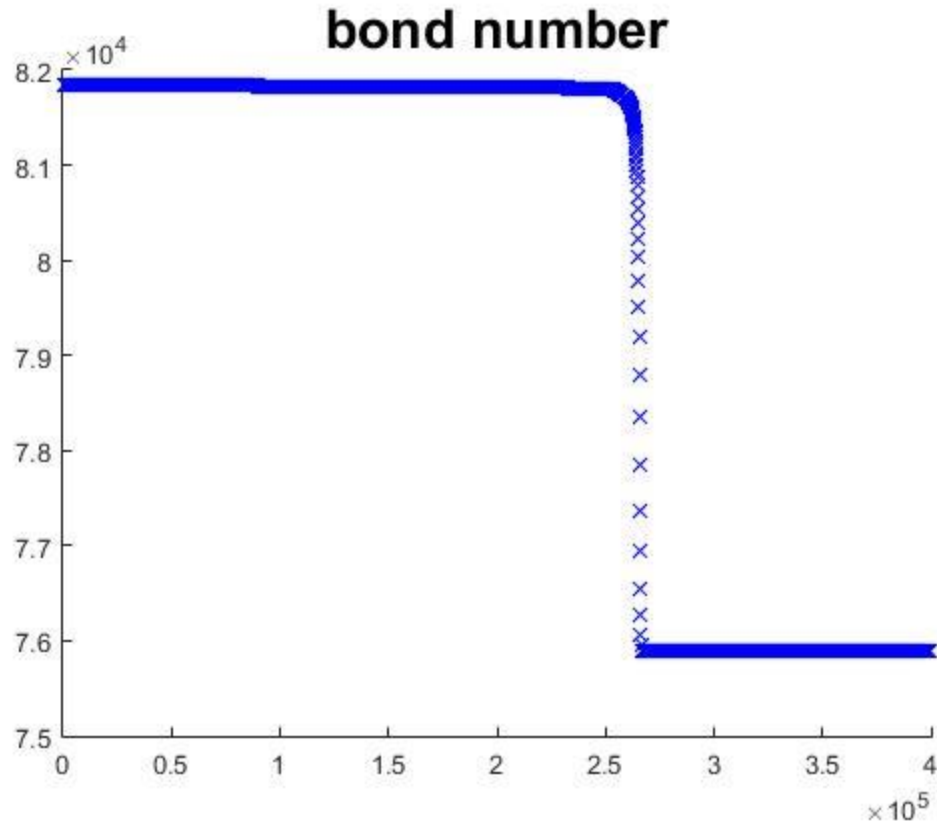


Figure 25 Bond number of double layer hydrogel under deformation. Recall the theoretical bond breaking probability P_b curve. This bond number profile is similar to the theoretical curve, which validate the applicability of the bond breaking model into the cross-linked polymeric system. If we take a look at Figure 25 and Figure 26, a large amount of bond breaking will always lead to an instant rise on system temperature. Comparing to the bulk sample, the more bonds are broken at a short period, the higher the temperature peak will be. And also, lower value of bond sensitivity gives higher temperature increasing. A less sensitive bond will break at a larger

external force and thus the velocity of two chain ends will be higher and leads to a higher temperature.

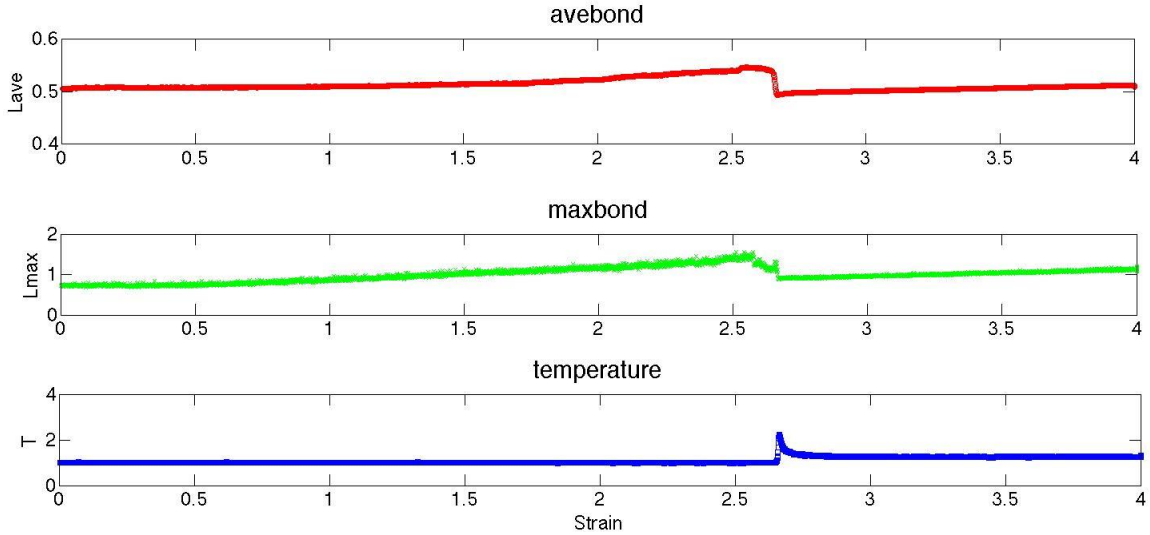


Figure 26 Bond length and temperature.

If we look at the maximum bond length curve around the strain of 250% more carefully in Figure 26, the fluctuation of this curve is more intense than the earlier stage. Because the spring-like harmonic bonds can frequently vibrate when they are elongated.

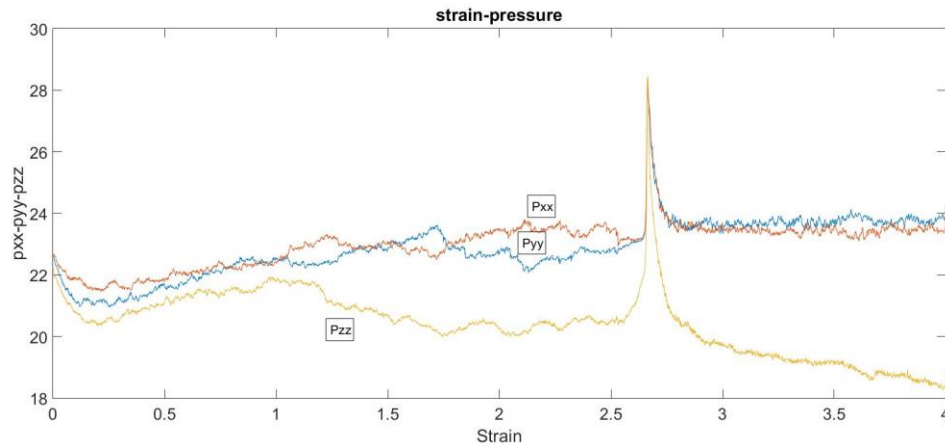


Figure 27 Pressure curve of hydrogel composites.

Recall the pressure equation for the I, J components.

$$P_{I,J} = \frac{\sum_k^N m_k v_{kI} v_{kJ}}{V} + \frac{\sum_k^N r_{kI} f_{kJ}}{V}$$

The pressure of the three direction all experience a rapid climbing because while the system loses a huge amount of bond interaction and recovers the pairwise interaction instantly, it need to expand to keep the same hydrostatic pressure. But the volume change is not instantaneous. So the system will have a period for the pressure to go down to the pre-set level with NPT (Slizberg & Andzelm, 2012). The sample is stretched in the z-direction and due to the incompressibility of hydrogel, the Poisson's ratio will be 0.5 and the sample will shrink in the other two directions respectively. That's why P_{zz} does not converge with P_{xx} and P_{yy} during the deformation.

We then check the density profile as shown in the figure below.

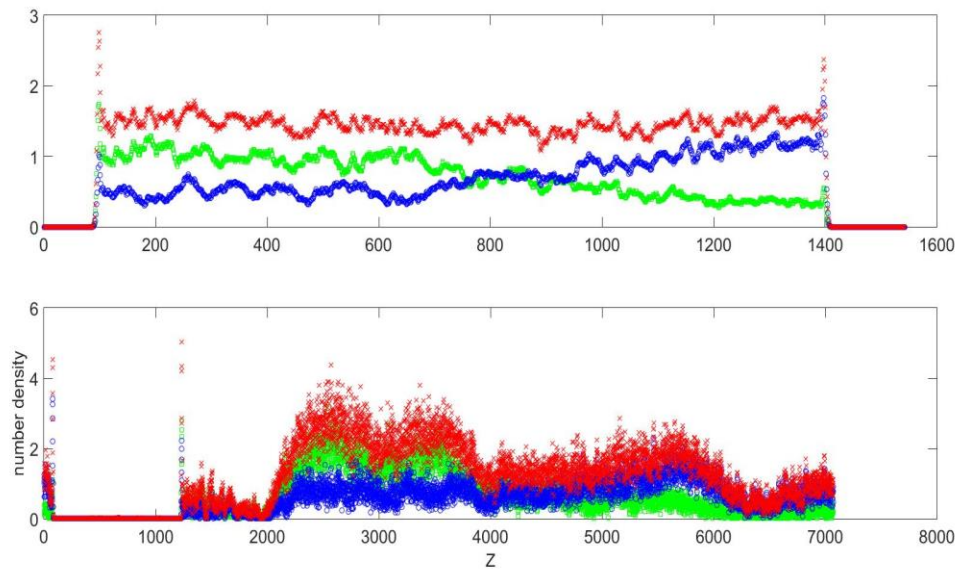


Figure 28 Density profile

The upper-side one is the density evolution profile of the original sample before deformation and fully relaxed. The second one is the final stage of the sample experienced deformation and fracture. Since all the sample we used in the simulation have periodic boundary condition, the sample will drift a bit during the deformation due to the asymmetry of the simulation box to the zero point. The red lines are the total number density of the two-layer composite. The green and blue lines represent the number density of each gel respectively. First thing first, we can see the interface of the composite hydrogel does not stay at the exact middle of the height. It moves upward a little after the gel reached equilibrium state because the mass of the species and the convection flow of the two gels (Jang, Goddard, & Kalani, 2007). After deformation and fracture, there appears obvious void areas at two end of the sample. The one close to the bottom has zero number density part which is the major fail part. And because the spring-like characteristic of the network, there is a high number density part right above the failure part. The number density there goes to about twice as the original one. This result meets the expect to this double network hydrogel. Although the two layers of gels are generated with the same species, they form a double network near the interface where they have very close number density. This double network made by cross-linked polymers is much tougher than the single

network gels. In addition, although not shown in this thesis, the low number density part near the top of the sample actually happens after the bottom area completely failed in the gif movie. So the real fracture and the first fracture is the bottom one. The one near the top could possibly be the necking effect of the material (Wv, 1995). If we keep stretching the simulation box, the top one will probably fail as well.

Then we want to check the strain-stress curve from the start of deformation to the failure of the material as shown in the figure below.

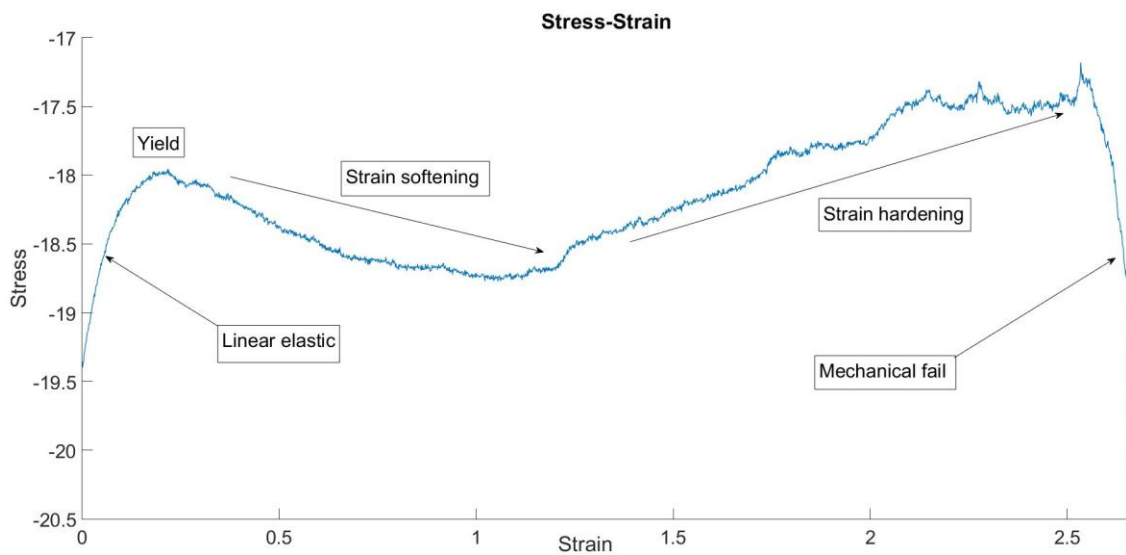


Figure 29 Strain-Stress curve

Since the stress is calculated by all the atoms in the simulation box including solvent, it does not start from 0 due to the pre-set pressure and the contribution from the solvent beads. The stress-strain relation of hydrogel actually acts like most materials. It has linear elastic regime, yield point, strain softening and strain hardening. The curve after the complete failure of

the material was taken out. It is not difficult to understand the elasticity of this rubber-like double network hydrogel. An amorphous polymer network with spring-like bond property should have linear elastic part because high molecular polymers follow the Hook's Law within small deformation (Yang et al., 2014). The freedom of movement of the polymer chains in the system is highly restricted by cross-linking and entanglement. But as the strain goes larger and larger, some of the unmovable chains will be drag out from its entanglement or separated out from the polymer network. That is why the material has a yield point. And the detachment process is irreversible. The separated chains do not have the ability to form entanglement or cross-linking back again under the same condition. Thus the hydrogel has strain softening regime. Also the participation of solvent will reinforce the strain softening of the material. After the strain softening, the material actually does not have real fracture in its polymer chains. The decrease of the stress curve is mainly due to the loss of entanglement. After the strain softening regime, the polymer chains are mostly stretched. So if we keep applying the strain. The material will again represent the ability to resist deformation. And in this so called "strain hardening regime", the resistance is mostly contributed by the chains themselves, through the covalent bonds (Lorenz et al., 2004). This can also explain why the average and maximum bond

distance do not have obvious upward curvature before the strain hardening regime. From this stress-strain curve, we can say that the strength provided by the covalent bonds are bigger than the physical entanglements because the highest point before fracture is higher than the yield point.

6. Conclusion

In this thesis project, we used LAMMPS as a simulation tool to implement the study of mechanical response of amorphous polymeric systems with dissipative particle dynamics. The major research object is an atom transfer radical polymerization (ATRP) regenerated two-layered double network hydrophilic gel. The reason we use DPD is this is a mesoscopic coarse-grained molecular dynamic algorithm between microscale (atomistic) and macroscale (MD) which is efficient and appropriate to my study object.

We first validate the fracture model of spring-like polymer chains formed by polymer beads and covalent bonds we introduced using a simplified single-chain sample. And select a suitable equilibrium ensemble (NPT) as the residual energy relaxation method. Then we apply the model to two different hydrophilic polymers. One is bulk polymer without cross-linking reaction which is more ductile. The other is a two-layered cross-linked hydrogel composite generated from a single layer hydrogel.

We found that the dominant component in the model of fracture is the bond sensitivity. When we choose a higher value of sensitivity, the bond breakage starts early (even at the beginning of the deformation) and the fast breaking

rate does not have detectable change. The whole sample represent the characteristic of polymer melts which is not appropriate. When the sensitivity is tuned to an acceptable value. The shape of bond number curve is very similar to the theoretical curve of bond breaking probability. A large amount of bonds breaks within a very short period (almost instantly) like the rupture of a very tense-stretched spring. The sudden rupture of the sample seems fine but it will also cause bad dynamics of the system because the bond breakage typically alters the system energy. Anything inducing a dramatic change in system energy will cause extraordinary temperature diversification which is recognized as bad dynamics at most time. We have to use thermostat to compensate for the system energy fluctuation due to the bond break. We could either tune the bond constant to make the bonds less stiff or increase the bond sensitivity to let the bonds break at lower external force. In addition, in order to remain the incompressibility of the hydrogel, we should use different pressure in the NPT ensemble before and after fracture because the huge loss of bond interactions will make the sample swell for a certain ratio. The two-layer hydrogel fracture model done in this thesis certainly has many atoms with very high velocity in the simulation box after bond breakage. This causes the high peak of the temperature curve. The temperature does not go back to the original level but stay higher than

that even after the NPT equilibrium. We can use smaller strain rate or smoother bond breaking process to avoid this. But in that case, obvious void in the polymer network will not be observed because the system will reach equilibrium states before the fracture part can be seen.

The two-layer cross-linked hydrogel composite, like most amorphous polymers, is flexible and can endure large deformation. In my simulation, the structure failure of the sample happens around 270% strain, almost three times the original length. Although it has notable ductility, the yield point appears pretty early during the deformation. And after the yield point, the material will lose its ability to recover to the original structure because the polymer chains will not entangle with each other again under the same situation.

Further research could be done like studying the mechanical response of this hydrogel with different bond constants, different strain rates. Or study the fracture behavior at lower temperature to see whether the hydrogel will represent more brittleness or not.

7. Reference

- Doerr, T. P., & Taylor, P. L. (1994). Breaking in polymer chains. I. The harmonic chain. *The Journal of Chemical Physics*, 101(1994), 10107–10117.
- Gao, H., Polanowski, P., & Matyjaszewski, K. (2009). Gelation in living copolymerization of monomer and divinyl cross-linker: Comparison of ATRP experiments with Monte Carlo simulations. *Macromolecules*, 42(16), 5925–5932.
- Groot, R. D., & Warren, P. B. (1997). Dissipative particle dynamics: Bridging the gap between atomistic and mesoscopic simulation. *The Journal of Chemical Physics*, 107(11), 4423.
- Iyer, B. V. S., Yashin, V. V., & Balazs, A. C. (2014). Dynamic behavior of dual cross-linked nanoparticle networks under oscillatory shear. *New Journal of Physics*, 16.
- Iyer, B. V. S., Yashin, V. V., Hamer, M. J., Kowalewski, T., Matyjaszewski, K., & Balazs, A. C. (2014). Ductility, toughness and strain recovery in self-healing dual cross-linked nanoparticle networks studied by computer simulations. *Progress in Polymer Science*, 40, 121–137.
- Jakobsen, A. F. (2005). Constant-pressure and constant-surface tension simulations in dissipative particle dynamics. *Journal of Chemical Physics*, 122(12).
- Jang, S. S., Goddard, W. a, & Kalani, M. Y. S. (2007). Mechanical and transport properties of the poly(ethylene oxide)-poly(acrylic acid) double network hydrogel from molecular dynamic simulations. *The Journal of Physical Chemistry. B*, 111(7),

1729–1737.

Lorenz, C. D., Stevens, M. J., & Wool, R. P. (2004). Fracture behavior of triglyceride-based adhesives. *Journal of Polymer Science, Part B: Polymer Physics*, 42(18), 3333–3343.

Martyna, G. J., Tobias, D. J., & Klein, M. L. (1994). Constant pressure molecular dynamics algorithms. *The Journal of Chemical Physics*, 101(September), 4177.

Meakin, P. (1991). Models for Material Failure and Deformation. *Science*, 252(5003), 226–234.

Polanowski, P., Jeszka, J. K., Li, W., & Matyjaszewski, K. (2011). Effect of dilution on branching and gelation in living copolymerization of monomer and divinyl cross-linker: Modeling using dynamic lattice liquid model (DLL) and Flory-Stockmayer (FS) model. *Polymer*, 52(22), 5092–5101.

Sliozberg, Y. R., & Andzelm, J. W. (2012). Fast protocol for equilibration of entangled and branched polymer chains. *Chemical Physics Letters*, 523, 139–143.

Snow, S. C., Yong, X., Kuksenok, O., & Balazs, A. C. (2015). Regenerating Composite Layers from Severed Nanorod-Filled Gels, 87–92.

Termonia, Y., Meakin, P., & Smith, P. (1985). Theoretical study of the influence of the molecular weight on the maximum tensile strength of polymer fibers. *Macromolecules*, 18(15), 2246–2252.

Thompson, A. P., Plimpton, S. J., & Mattson, W. (2009). General formulation of pressure

and stress tensor for arbitrary many-body interaction potentials under periodic boundary conditions. *Journal of Chemical Physics*, 131(15).

Trofimov, S. Y., Nies, E. L. F., & Michels, M. A. J. (2005). Constant-pressure simulations with dissipative particle dynamics. *Journal of Chemical Physics*, 123(14).

Wv, P. D. (1995). on Neck Propagation in Amorphous Glassy Polymers Under Plane Strain Tension, 11(3), 211–235.

Yang, S., Cui, Z., & Qu, J. (2014). A coarse-grained model for epoxy molding compound. *Journal of Physical Chemistry B*, 118(6), 1660–1669.

Yong, X., Kuksenok, O., & Balazs, A. C. (2015). Modeling free radical polymerization using dissipative particle dynamics. *Polymer*, 1–9.

Yong, X., Kuksenok, O., Matyjaszewski, K., & Balazs, A. C. (2013). Harnessing interfacially-active nanorods to regenerate severed polymer gels. *Nano Letters*, 13(12), 6269–6274.

Yong, X., Simakova, A., Averick, S., Gutierrez, J., & Kuksenok, O. (n.d.). Supporting Information Stackable , Covalently-Fused Gels : Repair and Composite Formation.

Yong, X., Simakova, A., Averick, S., Gutierrez, J., Kuksenok, O., Balazs, A. C., & Matyjaszewski, K. (2015). Stackable, covalently fused gels: Repair and composite formation. *Macromolecules*, 48(4), 1169–1178.